particles at large distances is described by the Yukawa potential.[7]

An inspection of the method used to obtain this result shows that it would also be obtained under more general conditions than those assumed here. If, in the Lagrangian density (1), the last term were replaced by some other function which also led to particle-like solutions, and which was negligible compared to the other terms at large distances from the particle center, then the same result would be obtained for the interaction, except for the numerical coefficient. For example, this would be the case if the last term were taken proportional to $(\psi\psi^*)^n$ for any $n>1$.

[7] H. Yukawa, Proc. Phys.-Math. Soc. Japan (3) **17**, 48 (1935).

PHYSICAL REVIEW VOLUME 85, NUMBER 2 JANUARY 15, 1952

Fine Structure of the Hydrogen Atom.* III

WILLIS E. LAMB, JR.†
Columbia Radiation Laboratory, Columbia University, New York, New York

(Received September 19, 1951)

The third paper of this series provides a theoretical basis for analysis of precision measurements of the fine structure of hydrogen and deuterium. It supplements the Bechert-Meixner treatment of a hydrogen atom by allowing for the presence of a magnetic field, as well as radiative corrections. The theory of hyperfine structure is somewhat extended. Stark effects due to motional and other electric fields are calculated. Possible radiative and nonradiative corrections to the shape and location of resonance peaks are discussed. Effects due to the finite size of the deuteron are also considered.

A theory of the sharp resonances $2^2S_{\frac{1}{2}}(m_s=\frac{1}{2})$ to $2^2S_{\frac{1}{2}}(m_s=-\frac{1}{2})$ is given which leads to an understanding of the peculiar shapes of resonance curves shown in Part II. In this connection, a violation of the "no-crossing" theorem of von Neumann and Wigner is exhibited for the case of decaying states.

THE earlier Parts[67] I and II of this paper have described some qualitative studies of the fine structure of hydrogen and deuterium made by a microwave method. In order to prepare the ground for analysis of much more highly precise measurements in Part IV, it is necessary to make available a more refined theory of the hydrogen atom than was used previously. The object of Part III is to supply this need, as well as to treat a number of other theoretical problems which arise in the work. Frequent references to Parts I and II are made. Chapters, sections, figures, tables, equations, and footnotes of Part III are numbered consecutively after those of Parts I and II.

J. ENERGY LEVELS OF A HYDROGEN-LIKE ATOM

48. General Program

The results of theory for the energy levels of an ideal hydrogen atom were given in Part I assuming an infinitely heavy nucleus, thereby neglecting reduced mass effects as well as magnetic and retarded interaction between electron and nucleus. In addition, a number of other approximations were made. The calculation of hyperfine structure was oversimplified by assumption of Back-Goudsmit and Russell-Saunders coupling. In the theories of Zeeman effect and doublet separation $P_{\frac{3}{2}}-P_{\frac{1}{2}}$ the anomalous magnetic moment of the electron was neglected. Shifts of levels due to Stark effect and relativistic and higher order corrections to Zeeman splitting were ignored.

There is no one place in the literature where a treatment of all these effects may be found. One may only form a patchwork Hamiltonian by collecting separate terms from papers by various authors who have been concerned with limited aspects of the problem. It would probably not be justified here to give a detailed systematic theory, but it does seem worthwhile to indicate the basis of the rather provisional treatment which is now possible. The object is to write down all terms known at present having a potential magnitude of 0.1 Mc/sec or larger in the discussion of the precision experiments of Part IV.

The electron and proton should be allowed to interact with one another through their intermediate coupling with the quantized electromagnetic field and the vacuum of occupied negative energy states for electrons and protons. By eliminating these effects from the theory, one hopes to find an equivalent two-body problem in which the two particles have a velocity and spin dependent interaction with one another, and the particles themselves have somewhat changed properties (renormalization of charge and mass, anomalous magnetic moments, etc.).

At present, this program has not been fully carried out. Those terms of low orders in the fine structure constant which have been found will be incorporated into the following discussion. It should be relatively easy to make the small corrections necessary when any missing terms have been calculated.

The starting point is here taken to be a two-body Dirac equation for electron and nucleus. Even when the nucleus is a proton and not a deuteron there might be grave doubt that it would obey an equation of the Dirac type in view of its anomalous magnetic moment.

* Work supported jointly by the Signal Corps and ONR.

† Present address: Department of Physics, Stanford University, Stanford, California.

[67] W. E. Lamb, Jr., and R. C. Retherford, Part I, Phys. Rev. **79**, 549 (1950), and Part II, **81**, 222 (1951).

If the additional magnetic moment is forced into the theory by insertion of terms[68] of the type used by Pauli, and if the calculation is not carried too far, it is possible to combine all terms referring to the magnetic moment of the proton so that only the observed moment enters the final equations. In this approximation it is reasonable to use the same result for other nuclei which do not even obey Fermi-Dirac statistics.

49. Two-Body Wave Equation

The two-body wave equation applicable to a hydrogen atom will be taken as

$$[H_1+H_2+e_1e_2/r+Y+\Omega+H(\text{h.f.})]\Psi=E\Psi \quad (103)$$

where

$$H_1=\boldsymbol{\alpha}_1\cdot(\mathbf{p}_1-e_1\mathbf{A}_1)+\beta_1m_1+e_1V_1, \quad \text{etc.} \quad (104)$$

where the index (1) refers to the electron and (2) to the proton. Relativistic units are used in which $\hbar$, c, and m are set equal to unity. Then $m_1=m=1$ and $m_2=M\sim1836$, and $e_1=-e$, $e_2=Ze$ while e^2 can be replaced by the fine structure constant $\alpha=e^2/\hbar c\sim1/(137.043)$. The wave function Ψ has $4\times4=16$ components $\Psi_{n_1n_2}$ where the Dirac matrices $\boldsymbol{\alpha}_1$, β_1 act on the first index $n_1=1$, 2, 3, 4 and $\boldsymbol{\alpha}_2$, β_2 act on the second index n_2. $\mathbf{A}$ and V are the vector and scalar potentials of the external electromagnetic field.

The interaction between the particles includes the Coulomb potential energy

$$U=e_1e_2/r \quad (105)$$

as well as the Breit[69]-Darwin[70] magnetic-retarded interaction

$$Y=-(e_1e_2/2r)[(\boldsymbol{\alpha}_1\cdot\boldsymbol{\alpha}_2)+(\boldsymbol{\alpha}_1\cdot\mathbf{r})(\boldsymbol{\alpha}_2\cdot\mathbf{r})/r^2]. \quad (106)$$

The finite remnants for a bound electron of the electromagnetic self-energy are represented by an operator Ω which allows for the anomalous magnetic moment of the electron and the electromagnetic level shift, etc.

The hyperfine energy term $H(\text{h.f.})$ is intended to represent only that part of the hyperfine interaction which arises from the non-Dirac part $\boldsymbol{\mu}_I'=\mu_I'\boldsymbol{\sigma}_2$ of the nuclear moment,

$$H(\text{h.f.})=-e_1\boldsymbol{\alpha}_1\cdot\mathbf{A}_I'(\mathbf{r}_1)-\mu_I'\boldsymbol{\sigma}_2\cdot\mathbf{H}(\mathbf{r}_2) \quad (107)$$

where

$$\mathbf{A}_I'=(\boldsymbol{\mu}_I'\times\mathbf{r})/r^3. \quad (108)$$

While the first three terms in the Hamiltonian (103) should be taken literally and treated exactly, it is known that this may not be done with Y which must in fact be evaluated using only first-order perturbation theory. This was established in 1929–1932 by Breit[69] in his discussion of the triplet fine structure of helium, and is connected with the omission of yet uncalculated fourth-order terms in e.

For similar reasons, or because of their smallness, the subsequent terms in the Hamiltonian will also be taken only in first order. This means that it suffices to calculate only

$$\bar{\Omega}=\int\Psi^*\Omega\Psi d\tau, \quad (109)$$

etc. where Ψ is the eigenfunction of the hydrogen atom with the Hamiltonian H_1+H_2+U without external fields. The solution of the underlying two-body Dirac equation is thereby much simplified, and subsequent calculation of the above averages is made fairly easy.

50. Reduction of Wave Equation

Two methods of approach have been used to solve the two-body Dirac equation. The first, used by Breit[69] and applied by Bechert and Meixner[71] to hydrogen fine structure, involved the reduction from a $4\times4=16$ component wave equation to a $2\times2=4$ component wave equation. Unfortunately, the treatment by Bechert and Meixner contains some errors which will be pointed out in the following discussion. More recently, Breit and Brown[72] gave a reduction to an 8 component wave equation. Both treatments led to the conclusion that the fine structure as calculated from the one-body Dirac equation was correct up to and including order α^2R except for the appearance of the reduced mass $\mu=mM/(m+M)$ in the expected manner and a common shift $\alpha^2R/(64M)$ for all $n=2$ levels.

The reduction to four components is used here because it permits a closer connection with the more elementary treatment given in Part I. Writing

$$\Psi=\begin{pmatrix}\phi\\ \omega_1\\ \omega_2\\ \chi\end{pmatrix}, \quad (110)$$

where the functions ϕ, ω_1, ω_2, and χ are four component wave functions with

$$\phi=\begin{pmatrix}\Psi_{11}\\ \Psi_{12}\\ \Psi_{21}\\ \Psi_{22}\end{pmatrix}, \quad \omega_1=\begin{pmatrix}\Psi_{31}\\ \Psi_{32}\\ \Psi_{41}\\ \Psi_{42}\end{pmatrix}, \quad \omega_2=\begin{pmatrix}\Psi_{13}\\ \Psi_{14}\\ \Psi_{23}\\ \Psi_{24}\end{pmatrix} \text{ and } \chi=\begin{pmatrix}\Psi_{33}\\ \Psi_{34}\\ \Psi_{43}\\ \Psi_{44}\end{pmatrix}. \quad (111)$$

[68] W. Pauli, Handbuch der Physik, second edition **24/1**, 233 (1933).
[69] G. Breit, Phys. Rev. **34**, 553 (1929); **39**, 616 (1932).
[70] C. G. Darwin, Phil. Mag. **39**, 537 (1920).
[71] K. Bechert and J. Meixner, Ann. Physik **22**, 525 (1935).
[72] G. Breit and G. E. Brown, Phys. Rev. **74**, 1278 (1948). Also, T. Ishidzu, Prog. Theor. Phys. **6**, 48 (1951).

we have

$$\boldsymbol{\alpha}_1\Psi=\boldsymbol{\sigma}_1\begin{pmatrix}\omega_1\\ \phi\\ \chi\\ \omega_2\end{pmatrix},\quad \beta_1\Psi=\begin{pmatrix}\phi\\ -\omega_1\\ \omega_2\\ -\chi\end{pmatrix},$$
$$\boldsymbol{\alpha}_2\Psi=\boldsymbol{\sigma}_2\begin{pmatrix}\omega_2\\ \chi\\ \phi\\ \omega_1\end{pmatrix}\quad\text{and}\quad \beta_2\Psi=\begin{pmatrix}\phi\\ \omega_1\\ -\omega_2\\ -\chi\end{pmatrix}, \tag{112}$$

where the σ's are four component spin matrices. The equation

$$[H_1+H_2+U-E]\Psi=0 \tag{113}$$

is then equivalent to the four equations

$$\begin{aligned}
&\boldsymbol{\sigma}_1\cdot(\mathbf{p}_1-e_1\mathbf{A}_1)\omega_1+\boldsymbol{\sigma}_2\cdot(\mathbf{p}_2-e_2\mathbf{A}_2)\omega_2\\
&\qquad+(m_1+m_2+U-E)\phi=0, \quad \text{(a)}\\
&\boldsymbol{\sigma}_1\cdot(\mathbf{p}_1-e_1\mathbf{A}_1)\phi+\boldsymbol{\sigma}_2\cdot(\mathbf{p}_2-e_2\mathbf{A}_2)\chi\\
&\qquad+(m_2-m_1+U-E)\omega_1=0, \quad \text{(b)}\\
&\boldsymbol{\sigma}_1\cdot(\mathbf{p}_1-e_1\mathbf{A}_1)\chi+\boldsymbol{\sigma}_2\cdot(\mathbf{p}_2-e_2\mathbf{A}_2)\phi\\
&\qquad+(m_1-m_2+U-E)\omega_2=0, \quad \text{(c)}\\
&\boldsymbol{\sigma}_1\cdot(\mathbf{p}_1-e_1\mathbf{A}_1)\omega_2+\boldsymbol{\sigma}_2\cdot(\mathbf{p}_2-e_2\mathbf{A}_2)\omega_1\\
&\qquad+(-m_1-m_2+U-E)\chi=0. \quad \text{(d)}
\end{aligned} \tag{114}$$

In reducing these equations to one for the large component ϕ, it is desirable to assign orders of magnitude in α and $1/M$ to the various terms. If the rest energy of the electron is taken as unity, that of the proton is $M\sim1836$, the Rydberg energy $hcRZ^2$ is $\frac{1}{2}\alpha^2Z^2$ and the fine structure doublet splitting for $n=2$ is $\frac{1}{16}\alpha^2Z^4R$ or $\frac{1}{32}\alpha^4Z^4\sim10{,}950$ Mc/sec for hydrogen. The radiative width of $2p$ is $(2^9/3^8)\alpha^3Z^4hcR$ or $(2/3)^8\alpha^5Z^4\sim99.7$ Mc/sec for $Z=1$, while the electromagnetic shift[73] of the $2^2S_{\frac{1}{2}}$ level for hydrogen is

$$\$\sim\frac{\alpha^5Z^4}{6\pi}\log(mc^2/Z^2\bar{\epsilon})\sim1040\text{ Mc/sec} \tag{115}$$

and abnormally large for its order because of the logarithm involving an atomic excitation energy $\bar{\epsilon}$. The term of order α^6 in the doublet separation, which according to Dirac's exact solution for hydrogen is $(5/256)\alpha^6\sim0.364$ Mc/sec, cannot be obtained even for the one-body problem by the method of reduction to two components, but this term may simply be borrowed from the exact treatment for $M=\infty$. Terms effectively of order α^6 due to an external magnetic field are correctly given by the subsequent treatment.

Turning now to terms in $1/M$, those of order α^2/M clearly correspond to reduced mass corrections to the Bohr energies. Any terms of orders α^3/M, α^4/M, α^5/M, and α^4/M^2 might be of importance for present microwave experiments, but calculation shows that of these only α^4/M and α^4/M^2 are actually present. Both have been examined, but the latter are numerically negligible, and for simplicity will be omitted in the subsequent discussion.

The Zeeman splitting in practice will be less than, but comparable to, the fine structure doublet splitting, so that the vector potential of the applied magnetic field will be overestimated if counted as of order given by

$$e_1\boldsymbol{\alpha}_1\cdot\mathbf{A}_1\sim\alpha^4/32\quad\text{or}\quad e_1A_1\sim\alpha^3/16 \tag{116}$$

with $eH_1\sim\alpha^4/16$. The Coulomb attraction

$$U=e_1e_2/r \tag{105}$$

has an average value of order $Z^2\alpha^2/4$, but for r equal to the classical electron radius $r_0=e^2/mc^2=\alpha$, U acquires the larger order unity so that terms involving it must be treated with more care. It may be remarked in passing that hyperfine splittings are of order α^4/M.

Taking ϕ of order unity, one sees that $\omega_1\sim\alpha$, $\omega_2\sim\alpha/M$, and $\chi\sim\alpha^2/M$. If the equation for ϕ derived from (114) is to be correct to order α^5/M, it is necessary that ω_1, and ω_2 be correctly calculated to order α^4/M. According to (114b) this requires that χ be known correctly to order α^3/M. From (114d), one obtains with this accuracy

$$\chi=(2M)^{-1}(\boldsymbol{\sigma}_2\cdot\mathbf{p}_2)\omega_1. \tag{117}$$

Likewise from (114c)

$$\omega_2=(2M-U+W)^{-1}[\boldsymbol{\sigma}_1\cdot(\mathbf{p}_1-e_1\mathbf{A}_1)\chi+\boldsymbol{\sigma}_2\cdot(\mathbf{p}_2-e_2\mathbf{A}_2)\phi], \tag{118}$$

where $W=E-M-1$ is the nonrelativistic energy, or to the requisite order

$$\omega_2=(2M)^{-1}\boldsymbol{\sigma}_2\cdot(\mathbf{p}_2-e_2\mathbf{A}_2)\phi \tag{119}$$

neglecting for $r\sim\alpha$ terms in ω_2 of order α/M^2 which slightly exceed the stated order α^3/M. However, a more careful consideration shows this neglect to be justified because of the small volume involved. Finally

$$\omega_1=(2-U+W)^{-1}[\boldsymbol{\sigma}_1\cdot(\mathbf{p}_1-e_1\mathbf{A}_1)\phi+\boldsymbol{\sigma}_2\cdot\mathbf{p}_2\chi]. \tag{120}$$

Insertion of these expressions in (114a) gives

$$\begin{aligned}
&\boldsymbol{\sigma}_1\cdot(\mathbf{p}_1-e_1\mathbf{A}_1)(2M+U+W)^{-1}[\boldsymbol{\sigma}_1\cdot(\mathbf{p}_1-e_1\mathbf{A}_1)\\
&\quad+(2M)^{-1}(\boldsymbol{\sigma}_2\cdot\mathbf{p}_2)^2(2-U+W)^{-1}\boldsymbol{\sigma}_1\cdot\mathbf{p}_1]\phi\\
&\quad+(2M)^{-1}\boldsymbol{\sigma}_2\cdot(\mathbf{p}_2-e_2\mathbf{A}_2)\boldsymbol{\sigma}_2\cdot(\mathbf{p}_2-e_2\mathbf{A}_2)\phi\\
&\qquad+(U-W)\phi=0.
\end{aligned} \tag{121}$$

After some reduction, keeping terms of order up to and including α^5/M and replacing $W-U$ by $\frac{1}{2}\mathbf{p}_1^2+\frac{1}{2}(\mathbf{p}_2^2/M)$ in terms of order α^4, one finds a wave equation for ϕ

$$(H_I+H_{II}+H_{III})\phi=W\phi \tag{122}$$

where the Hamiltonian

$$\begin{aligned}
H_I=&\tfrac{1}{2}\mathbf{p}_1^2-\tfrac{1}{8}\mathbf{p}_1^4+(\boldsymbol{\nabla}U\cdot\mathbf{p}_1)/4i\\
&+(2-U+W)^{-2}\boldsymbol{\sigma}_1\cdot\boldsymbol{\nabla}_1U\times\mathbf{p}_1+U
\end{aligned} \tag{123}$$

[73] H. A. Bethe, Phys. Rev. **72**, 339 (1947).

is familiar from the reduction[74] of the one-body Dirac equation to 2-component form, and for a hydrogen-like atom with fixed point nucleus gives the fine structure correctly to order α^4. The term

$$H_{II}=\tfrac{1}{2}(\mathbf{p}_2^2/M) \tag{124}$$

gives the kinetic energy of the nucleus, while

$$\begin{aligned}H_{III}=&-(2-U+W)^{-1}(2e_1\mathbf{A}_1\cdot\mathbf{p}_1+e_1\boldsymbol{\sigma}_1\cdot\mathbf{H}_1)\\&+\tfrac{1}{2}e_1^2\mathbf{A}_1^2-(2M)^{-1}(2e_2\mathbf{A}_2\cdot\mathbf{p}_2+e_2\boldsymbol{\sigma}_2\cdot\mathbf{H}_2)\\&+(e_1i/4)(\boldsymbol{\sigma}_1\cdot\boldsymbol{\nabla}U)(\boldsymbol{\sigma}_1\cdot\mathbf{A}_1)\end{aligned} \tag{125}$$

gives the interaction of the atom with an external magnetic field, except for some terms from Ω and H(h.f.) which are inserted later.

The energy contributed by the Darwin-Breit term Y is given by the average

$$\bar{Y}=-\tfrac{1}{2}e_1e_2\int\begin{pmatrix}\phi\\ \omega_1\\ \omega_2\\ \chi\end{pmatrix}^*\left[\frac{\boldsymbol{\sigma}_1\cdot\boldsymbol{\sigma}_2}{r}+\frac{\boldsymbol{\sigma}_1\cdot\mathbf{r}\boldsymbol{\sigma}_2\cdot\mathbf{r}}{r^3}\right]\begin{pmatrix}\chi\\ \omega_2\\ \omega_1\\ \phi\end{pmatrix}d\tau \tag{126}$$

which to the required order α works out to be just the average of the operator

$$\begin{aligned}H_{IV}=&[e_1e_2/(4M)][(\boldsymbol{\sigma}_1\cdot\boldsymbol{\sigma}_2)/r^3-3(\boldsymbol{\sigma}_1\cdot\mathbf{r})(\boldsymbol{\sigma}_2\cdot\mathbf{r})/r^5]\\&-[e_1e_2/(8M)](1+\tfrac{1}{2}\alpha/r)^{-2}r^{-2}\frac{dU}{dr}\\&\times[\boldsymbol{\sigma}_1\cdot\boldsymbol{\sigma}_2-(\boldsymbol{\sigma}_1\cdot\mathbf{r}\boldsymbol{\sigma}_2\cdot\mathbf{r}/r^2)]\\&-[e_1e_2/(2M)][r^{-1}\mathbf{p}_1\cdot\mathbf{p}_2+r^{-3}\mathbf{r}\cdot\mathbf{p}_1'\mathbf{r}\cdot\mathbf{p}_2']\\&-[e_1e_2/(2Mr^2)][\boldsymbol{\sigma}_2\cdot\mathbf{r}\times\mathbf{p}_1-\boldsymbol{\sigma}_1\cdot\mathbf{r}\times\mathbf{p}_2]\end{aligned} \tag{127}$$

for the state whose wave function is ϕ. The prime on $\mathbf{p}'$ indicates that the operator does not act on $\mathbf{r}$.

51. Exhibition of Reduced Mass

Bechert and Meixner[71] showed that when $\mathbf{p}_1=-\mathbf{p}_2=\mathbf{p}$ the Hamiltonian

$$H_I+H_{II}+H_{IV}$$

could be rearranged so as to exhibit explicitly the reduced mass μ by writing

$$H_I+H_{II}+H_{IV}=H_a+H_b+H_c, \tag{128}$$

where

$$\begin{aligned}H_a=&\mathbf{p}^2/(2\mu)-\mathbf{p}^4/(8\mu^3)+(\boldsymbol{\nabla}U\cdot\mathbf{p})/(4i\mu^2)\\&+\mu^{-2}(2-U+W)^{-2}\boldsymbol{\sigma}_1\cdot\boldsymbol{\nabla}U\times\mathbf{p}+U\end{aligned} \tag{129}$$

is the Hamiltonian of type (123) for a particle of mass μ.

[74] See, for example, L. I. Schiff, *Quantum Mechanics* (McGraw-Hill Book Company, Inc., New York, 1949), p. 320.

52. Fine and Hyperfine Energies

The remaining terms from

$$H_I+H_{II}+H_{IV}$$

may be written as

$$\begin{aligned}H_b=&(3/8M)\mathbf{p}^4-(\boldsymbol{\nabla}U\cdot\mathbf{p})/(2iM)\\&+(e_1e_2/2M)(r^{-1}\mathbf{p}^2+r^{-3}\mathbf{r}\cdot\mathbf{p}'\mathbf{r}\cdot\mathbf{p}')\end{aligned} \tag{130}$$

and

$$\begin{aligned}H_c=&(e_1e_2/4M)[r^{-3}\boldsymbol{\sigma}_1\cdot\boldsymbol{\sigma}_2-3r^{-5}\boldsymbol{\sigma}_1\cdot\mathbf{r}\boldsymbol{\sigma}_2\cdot\mathbf{r}]\\&-[e_1e_2/(2Mr)](\boldsymbol{\sigma}_2\cdot\mathbf{r}\times\mathbf{p}_1)-[e_1e_2/(8M)]\\&\times(r+\tfrac{1}{2}\alpha)^{-2}\frac{dU}{dr}(\boldsymbol{\sigma}_1\cdot\boldsymbol{\sigma}_2-r^{-2}\boldsymbol{\sigma}_1\cdot\mathbf{r}\boldsymbol{\sigma}_2\cdot\mathbf{r}).\end{aligned} \tag{131}$$

H_c gives contributions to the hyperfine energy and will be considered further in Sec. 56.

The above equations are equivalent to those used by Bechert and Meixner, except that their terms containing

$$\boldsymbol{\nabla}U\cdot\mathbf{p}$$

in H_a and H_b have the wrong sign. These errors are compensated by their use of incorrect expressions for the averages of $\mathbf{p}^4$

$$(r^{-1}p^2+r^{-3}\mathbf{r}\cdot\mathbf{p}'\mathbf{r}\cdot\mathbf{p}')$$

which in fact have the values for the nl state of hydrogen of

$$(\mathbf{p}^4)_{\text{Av}}=(-3+4n/(l+\tfrac{1}{2}))(\alpha^4/n^4) \tag{132a}$$

$$\begin{aligned}&(r^{-1}\mathbf{p}^2+r^{-3}\mathbf{r}\cdot\mathbf{p}'\mathbf{r}\cdot\mathbf{p}')_{\text{Av}}\\&\quad=(-2+3n/(l+\tfrac{1}{2})-2n\delta_{l0})(\alpha^3/n^4).\end{aligned} \tag{132b}$$

Also

$$(\boldsymbol{\nabla}U\cdot\mathbf{p})/i=e_1e_2(r^{-2}\partial/\partial r)_{\text{Av}}=(2\alpha^4/n^3)\delta_{l0}. \tag{132c}$$

The discrepancies between these values and those of Bechert and Meixner arise because the results depend on whether or not a small sphere about $r=0$ is excluded. In the above equations, care has been taken to find the correct interpretation for the singularities. No sphere is to be excluded in (132a), but must be for (132b). The result is then that H_b has the same average value

$$-\alpha^4/(8Mn^4)$$

for all the fine structure levels for a given n, and therefore the separations predicted by H_a are not disturbed. Although this result was derived by treating the nucleus as a particle obeying Dirac's equation, it is clearly more general, and should follow to order α^4/M from any relativistic treatment of the two-body problem. The first two terms of H_b enter to compensate for the forcing of the reduced mass μ into H_a in the manner in which it would appear if the one-body Dirac equation for a particle of mass μ were reduced to two-component form. This is done merely for convenience in calculation. The last term in H_b is just the Darwin retarded-magnetic

interaction energy which has a classical analog for any distribution of currents.

In the following sections are given the detailed expressions which make up the working Hamiltonian for analysis of the experiments. These include: unperturbed energies, Zeeman, hyperfine, and Stark energies.

K. WORKING HAMILTONIAN

53. Unperturbed Levels

In the absence of an external electric field (motional or otherwise), there are no terms in the Hamiltonian which mix S and P states. This is true both for hyperfine interaction and electromagnetic term shift Ω. The unperturbed states in the absence of hyperfine and Zeeman splitting may be specified by quantum numbers n, j, m_j for the electron which are indicated in Table II. with energies 0, $\mathcal{S}$, and ΔE shown in Fig. 47. Quantum numbers I and m_I for the nuclear spin will also be used.

The position of $2^2P_{\frac{1}{2}}$ is taken as the zero of energy for convenience despite the fact that the absolute position of $2^2P_{\frac{1}{2}}$ is changed by the quantum electrodynamic effects. According to Dirac's treatment, $\mathcal{S}=0$ and with inclusion of the reduced mass where it is significant

$$\Delta E=(1/32)\mu\alpha^4+(5/256)\alpha^6. \tag{133}$$

The electrodynamic shifts of levels δE_{nlj} which arise from Ω may be written as[75,76]

$$\begin{aligned}\delta E_{20\frac{1}{2}}&=(\alpha^5/6\pi)[\log(1/2k_0)+19/30],\\ \delta E_{21\frac{1}{2}}&=(\alpha^5/6\pi)[\log(\alpha^2/2k_1)-1/8],\\ \delta E_{21\frac{3}{2}}&=(\alpha^5/6\pi)[\log(\alpha^2/2k_1)+1/16],\end{aligned} \tag{134}$$

where k_0 and k_1 are average atomic excitation energies. One gets thereby an additional contribution to ΔE of $\alpha^5/(32\pi)$ or 25.40 Mc/sec due to the spin-orbit interaction association with the second-order anomalous magnetic moment[77] $(\alpha/2\pi)\mu_0$ of the electron. When the 1.38 percent fourth-order[78] reduction in this moment is included, ΔE becomes

$$\begin{aligned}\Delta E=&(1/32)\mu\alpha^4+(5/256)\alpha^6\\ &+(\alpha^5/32\pi)(1-5.946(\alpha/\pi)).\end{aligned} \tag{135}$$

Using the 1951 constants of Bearden and Watts[79] $\Delta E/h$ is

$$\Delta E/h=\begin{cases}10{,}967.463\text{ Mc/sec for }H\\ 10{,}970.447\text{ Mc/sec for }D.\end{cases} \tag{136}$$

The relative level shift $\mathcal{S}$ according to Eq. (134) is

$$\mathcal{S}=(\alpha^5/6\pi)\left[\log\left(\frac{k_1}{\alpha^2k_0}\right)+\frac{19}{30}+\frac{1}{8}\right] \tag{137}$$

TABLE II. Unperturbed energy levels.

	n	l	j	m_j	Energy
$2^2S_{\frac{1}{2}}$	2	0	$\frac{1}{2}$	$\pm\frac{1}{2}$	$E^0(2^2S_{\frac{1}{2}})=\mathcal{S}$
$2^2P_{\frac{1}{2}}$	2	1	$\frac{1}{2}$	$\pm\frac{1}{2}$	$E^0(2^2P_{\frac{1}{2}})=0$
$2^2P_{\frac{3}{2}}$	2	1	$\frac{3}{2}$	$\pm\frac{3}{2}$, $\pm\frac{1}{2}$	$E^0(2^2P_{\frac{3}{2}})=\Delta E$

which should be 1051.41 Mc/sec for hydrogen according to Bethe, Brown and Stehn.[75] The second-order anomalous electron magnetic moment contributes 67.77 Mc/sec of this. When the effect of the subsequently calculated fourth-order magnetic moment is included, the shift becomes 1050.47 Mc/sec. According to the above authors,[75] the shift ought to be proportional[80] to the electronic reduced mass μ, which would make it 0.29 Mc/sec higher for deuterium.

There appears to be an unexplained discrepancy between this value and the previously reported[67] value for $\mathcal{S}$ of 1062±5 Mc/sec. In any case, the object of the present research is to determine an experimental value for $\mathcal{S}$, and the reduction of data is entirely independent of its theoretical value.

54. Magnetic Energy

The contribution of H_{III} is given by

$$(H_{III})_{Av}=\int\phi^*H_{III}\phi d\tau \tag{138}$$

in which terms smaller than the usual Zeeman energy by factors $1/M$ and α^2 are to be kept. The latter requires that departures of ϕ of order α^2 from the usual nonrelativistic Schrödinger wave function be considered. These might be of two kinds: (1) a mixing of other states and (2) a renormalization. Fortunately only the latter gives a contribution. One has

$$\int(|\phi|^2+|\omega_1|^2)d\tau\sim 1$$

or

$$\int|\phi|^2d\tau\sim 1-\tfrac{1}{4}(p^2)_{Av}=1+\tfrac{1}{2}W \tag{139}$$

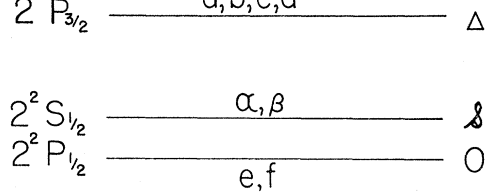

FIG. 47. Energy levels for $2^2S_{\frac{1}{2}}$ in zero magnetic field without hyperfine structure. The magnetic sub-levels are indicated by letters α, β, a, b, c, d, e, and f as in Fig. 14.

[75] Bethe, Brown, and Stehn, Phys. Rev. **77**, 370 (1950).
[76] E. R. Cohen, report to be published.
[77] J. Schwinger, Phys. Rev. **73**, 416 (1948).
[78] R. Karplus and N. M. Kroll, Phys. Rev. **77**, 536 (1950).
[79] J. A. Bearden and H. M. Watts, Phys. Rev. **81**, 73 (1951).
[80] Bethe, Brown, and Stehn did not consider radiative processes involving the nucleus. Unpublished calculations by B. S. Gourary which take these into account indicate a somewhat larger dependence on reduced mass.

TABLE III. Coefficients of Eq. (143) for various states.

State	α	β	a	b	c	d	e	f
Coefficient	7/36	7/36	6/36	4/36	4/36	6/36	5/36	5/36

where the nonrelativistic energy is

$$W=-\alpha^2/8 \tag{140}$$

for $n=2$. Then H_{III} is equivalent to the average of the operator

$$\begin{aligned}H_{III}\rightarrow&-\tfrac{1}{2}(2e_1\mathbf{A}_1\cdot\mathbf{p}_1+e_1\boldsymbol{\sigma}_1\cdot\mathbf{H}_1)\\&-\tfrac{1}{2}(2e_2\mathbf{A}_2\cdot\mathbf{p}_2+e_2\boldsymbol{\sigma}_2\cdot\mathbf{H}_2)/M\\&+\tfrac{1}{2}e_1^2\mathbf{A}_1^2+W\mu_0(\mathbf{L}+2\mathbf{S})\cdot\mathbf{H}\\&+\tfrac{1}{8}(\boldsymbol{\sigma}_1\cdot\boldsymbol{\nabla}U)\cdot(\mathbf{H}\times\mathbf{r})\end{aligned} \tag{141}$$

calculated with the usual Schrödinger wave function, where $\mu_0=\frac{1}{2}(\alpha)^{\frac{1}{2}}$ is the Bohr magneton. The term $e_2\boldsymbol{\sigma}_2\cdot\mathbf{H}/8M$ will be treated with other contributions to hyperfine energy in Sec. 56.

(a) *Relativistic Corrections to Magnetic Moment*

The last two terms of (141), in case of Russell-Saunders coupling, are equivalent to the relativistic corrections of order α^2 to the magnetic moment of the atom as first calculated by Breit.[81] According to these, the effective Landé g-values for the various states are given by

$$g_j=g_j^{(0)}\begin{cases}1+\frac{2}{3}W & 2^2S_{\frac{1}{2}}\\ 1+2W & 2^2P_{\frac{1}{2}},\\ 1+\frac{4}{5}W & 2^2P_{\frac{3}{2}}\end{cases} \tag{142}$$

where

$$g_j^{(0)}=2,\ \tfrac{2}{3},\text{ and }4/3 \tag{142a}$$

for these states, respectively. For a magnetic field of 1500 gauss, larger than those used in the precision determinations of Part IV, the correction to the frequency of transition $\alpha\beta$ amounts to only 0.02 Mc/sec, and is no larger for any other transition. The relativistic moment corrections may therefore be neglected, although they are of the retained order α^6.

(b) *Quadratic Zeeman Energy*

The quadratic Zeeman energy is likewise too small to require a correction, although also of nominal order α^6. Thus for $2^2S_{\frac{1}{2}}$

$$\begin{aligned}(\tfrac{1}{2}e_1^2\mathbf{A}_1^2)_{Av}&=\tfrac{1}{8}e^2H^2(r^2\sin^2\theta)_{Av}=(7/2)e^2a_0^2H^2\\&=7(\mu_0H)^2/(hcR)=(7/36)\alpha^2x^2\Delta E\end{aligned} \tag{143}$$

which for $H=1500$ gauss amounts to 0.01 Mc/sec. The values of the coefficient of $\alpha^2x^2\Delta E$ in Eq. (143) for the other Zeeman components, assuming Russell-Saunders coupling, are given in Table III.

[81] G. Breit; Nature **122**, 649 (1928), also Mott and Massey, *Theory of Atomic Collisions* (Oxford University Press, London, 1933), first edition, pp. 47–57; H. Margenau, Phys. Rev. **57**, 383 (1940).

(c) *Energy of Orientation of Electron Spin*

To the term $-\frac{1}{2}e_1\boldsymbol{\sigma}_1\cdot\mathbf{H}_1$ in (141) must be added the contribution from Ω of the anomalous magnetic moment of the electron, giving in usual units an orientation energy

$$g_S\mu_0\mathbf{S}\cdot\mathbf{H} \tag{144}$$

where the Landé g-factor is[77,78]

$$g_S=2(1+(\alpha/2\pi)-2.973\alpha^2/\pi^2). \tag{145}$$

(d) *Reduced Mass Effects and Motional Electric Field*

The remaining terms of H_{III} are

$$H_{III}'=-(e_1/m_1)\mathbf{A}_1\cdot\mathbf{p}_1-(e_2/m_2)\mathbf{A}_2\cdot\mathbf{p}_2. \tag{146}$$

It will be shown how these terms imply the introduction of an effective g value for orbital motion

$$g_L=1-(1/M) \tag{146a}$$

and also contribute an electric field due to motion of the atom through a uniform magnetic field. The vector potentials are then

$$\mathbf{A}_1=\tfrac{1}{2}\mathbf{H}\times\mathbf{r}_1,\quad \mathbf{A}_2=\tfrac{1}{2}\mathbf{H}\times\mathbf{r}_2 \tag{147}$$

so that (146) becomes

$$\begin{aligned}H_{III}'=-\tfrac{1}{2}[&(e_1/m_1)(\mathbf{H}\cdot\mathbf{r}_1\times\mathbf{p}_1)\\&+(e_2/m_2)(\mathbf{H}\cdot\mathbf{r}_2\times\mathbf{p}_2)]\end{aligned} \tag{148}$$

and upon transformation to relative and center-of-mass coordinates by the equations

$$\begin{aligned}&\mathbf{r}=\mathbf{r}_1-\mathbf{r}_2,\quad \mathfrak{M}\mathbf{R}=m_1\mathbf{r}_1+m_2\mathbf{r}_2,\quad \mathfrak{M}=m_1+m_2\\&\mathbf{p}_1=(m_1/\mathfrak{M})\mathbf{P}+\mathbf{p}\quad \mathbf{p}_2=(m_2/\mathfrak{M})\mathbf{P}-\mathbf{p}\end{aligned} \tag{149}$$

becomes

$$\begin{aligned}H_{III}'=&-(2\mathfrak{M})^{-1}(e_1+e_2)[\mathbf{H}\cdot\mathbf{R}\times\mathbf{P}]\\&-\tfrac{1}{2}(e_1m_1^{-1}-e_2m_2^{-1})(\mathbf{H}\cdot\mathbf{R}\times\mathbf{p})\\&-\tfrac{1}{2}(e_1m_2-e_2m_1)\mathfrak{M}^{-2}(\mathbf{H}\cdot\mathbf{r}\times\mathbf{P})\\&-\tfrac{1}{2}(e_1m_2m_1^{-1}+e_2m_1m_2^{-1})\mathfrak{M}^{-1}(\mathbf{H}\cdot\mathbf{r}\times\mathbf{p}).\end{aligned} \tag{150}$$

The first term is zero for a neutral atom with $e_1=-e_2$, and the last term in usual units is

$$g_L\mu_0\mathbf{H}\cdot\mathbf{L}, \tag{151}$$

where

$$\mathbf{L}=\mathbf{r}\times\mathbf{p} \tag{152}$$

is the orbital angular momentum operator, and

$$g_L=m_1^{-1}-m_2^{-1}=1-(1/M) \tag{153}$$

as stated above. Needless to say, this result can also be obtained by more elementary methods.

The third term of (150) may be written as

$$-\tfrac{1}{2}e_1(\mathbf{V}\times\mathbf{H}\cdot\mathbf{r}), \tag{154}$$

where

$$\mathbf{V}=\mathbf{P}/\mathfrak{M} \tag{155}$$

is the velocity of the atom, and represents just half of the expected Stark perturbation due to a motional electric field

$$\mathbf{E}=(\mathbf{V}\times\mathbf{H})/c. \tag{156}$$

This defect is made up by the second term of (150) which can be written as

$$-(e_1/\mu)\mathfrak{A}\cdot\mathbf{p} \tag{157}$$

with

$$\mathfrak{A}=\tfrac{1}{2}\mathbf{H}\times\mathbf{R} \tag{158}$$

the vector potential at the atomic center of mass $\mathbf{R}$. As far as the internal motion alone is concerned, this term is equivalent to a gauge transformation. Consider the wave equation for the atom

$$[\mathbf{P}^2/(2\mathfrak{M})+\mathbf{p}^2/(2\mu)-(e_1/\mu)\mathfrak{A}\cdot\mathbf{p}+g_L\mu_0\mathbf{L}\cdot\mathbf{H} -\tfrac{1}{2}e_1\mathbf{H}\cdot\mathbf{r}\times(\mathbf{P}/\mathfrak{M})+\cdots-W]\psi_1=0. \tag{159}$$

The gauge term containing

$$\mathfrak{A}=\mathrm{grad}_r(\mathfrak{A}\cdot\mathbf{r}) \tag{160}$$

may be removed by the transformation

$$\psi_1=\psi\exp(e_1 i/2\hbar)[\mathbf{H}\times\mathbf{R}\cdot\mathbf{r}]. \tag{161}$$

The operator $\mathbf{p}^2/2\mu$ acting upon ψ_1 gives an extra term which just cancels out the gauge term, while $\mathbf{P}^2/2\mathfrak{M}$ gives an additional contribution which doubles the motional Stark term. To first order in H, the result is

$$[\mathbf{P}^2/(2\mathfrak{M})+\mathbf{p}^2/(2\mu)-(e_1/\mathfrak{M})(\mathbf{P}\times\mathbf{H}\cdot\mathbf{r}) +g_L\mu_0\mathbf{H}\cdot\mathbf{L}+\cdots-W]\psi=0 \tag{162}$$

leading to the correct motional Stark effect.

55. Zeeman Energy

To summarize the results thus far, the Zeeman splitting is determined by the Hamiltonian

$$\mathcal{S}\delta_{l0}+\tfrac{2}{3}\Delta E(\mathbf{L}\cdot\mathbf{S}+\delta_{l1})+g_S\mu_0\mathbf{S}\cdot\mathbf{H}+g_L\mu_0\mathbf{L}\cdot\mathbf{H} \tag{163}$$

and the energy levels for the states $nljm_j$ may be written in a form similar to that given in Sec. 15

$$y_{\alpha,\beta}=y_0\pm x_\alpha, \tag{164}$$

$$y_{a,d}=\tfrac{3}{2}\pm 2x_a, \tag{165}$$

$$y_{b,c}=\tfrac{3}{4}\pm\tfrac{1}{2}x+\tfrac{1}{2}(x^2\pm x+(9/4))^{\frac{1}{2}}\pm\tfrac{1}{2}Tx, \tag{166}$$

$$y_{e,f}=\tfrac{3}{4}\pm\tfrac{1}{2}x-\tfrac{1}{2}(x^2\pm x+(9/4))^{\frac{1}{2}}\pm\tfrac{1}{2}Tx \tag{167}$$

with

$$T=(2g_L-g_S)/(g_S-g_L), \tag{168}$$

where the unit of y for all states is

$$f_1=\tfrac{2}{3}(\Delta E/h) \tag{169}$$

and

$$\mathcal{S}=f_1 y_0$$

while the units for the x's are given by

$$\text{Unit field for } x_\alpha\colon\ H_{1\alpha}=(2/g_S)(\tfrac{2}{3}\Delta E/\mu_0), \tag{170}$$

$$\text{Unit field for } x_a\colon\ H_{1a}=[2/(g_L+\tfrac{1}{2}g_S)](\tfrac{2}{3}\Delta E/\mu_0), \tag{171}$$

$$\text{Unit field for } x\colon\ H_1=[1/(g_S-g_L)](\tfrac{2}{3}\Delta E/\mu_0). \tag{172}$$

The values of these and other needed units using 1951 constants of Bearden and Watts[79] are given in Table IV.

In Eqs. (164)–(172) both $\mathcal{S}$ and ΔE are to be determined from observations of resonance peaks. This is inconvenient since the units of magnetic field depend on $\Delta E/\mu_0$. Fortunately the experimental value determined for $\mathcal{S}$ is highly independent of the values used for ΔE, μ_0, and h (strictly so except for nonlinearity of the Zeeman energy curves), so the procedure will be to regard $\Delta E/h$ as given by Eq. (136), and to determine $\mathcal{S}$ from the low frequency transitions αe and αf. Then the high frequency transitions αa, αb, αc may be used to determine a value for the fine structure constant, assuming validity of Eq. (136). If necessary the process can be iterated should the originally assumed value of ΔE prove to be in error.

56. Hyperfine Energy

The operator for the hyperfine energy is

$$w=g_I\mu_0^2(1+\tfrac{1}{2}(\alpha/r))r^{-3}[2\mathbf{I}\cdot\mathbf{L}-g_S(\mathbf{I}\cdot\mathbf{S}-3\mathbf{I}\cdot\mathbf{r}\mathbf{S}\cdot\mathbf{r}/r^2)] +2g_S g_I\mu_0^2(r+\tfrac{1}{2}\alpha)^{-2}(dU/dr) \times[\mathbf{I}\cdot\mathbf{S}-\mathbf{I}\cdot\mathbf{r}\mathbf{S}\cdot\mathbf{r}/r^2] \tag{173}$$

which agrees with (131) except for insertion of the observed g-values for nuclear and electronic spin. Such corrections arise from terms in Ω giving the interaction of anomalous part of the magnetic moment of the electron with the nuclear magnetic moment. In evaluation of this, as usual, S states require a special consideration. There are no matrix elements of w connecting S and P states, and it therefore suffices to consider only diagonal elements for a given l value w_{ll} which have been calculated by Bethe.[82]

(a) *S States*

For $l=0$, w_{00} reduces to Eq. (48) with an additional factor $g_S/2$, if some terms of relative order α^2 are neglected. In the presence of a magnetic field, the effective Zeeman-hyperfine Hamiltonian is

$$\mathcal{H}=\mathcal{S}+g_S\mu_0\mathbf{S}\cdot\mathbf{H}+\Delta w(I+\tfrac{1}{2})^{-1}\mathbf{I}\cdot\mathbf{S}-g_S\mu_0\mathbf{I}\cdot\mathbf{H} \tag{174}$$

where Δw is the hyperfine splitting for $2^2S_{\frac{1}{2}}$ produced by the nucleus in question (taken to be $\frac{1}{8}$ the corresponding value measured[83] for $1^2S_{\frac{1}{2}}$) given in Table IV.

In Part I the energy levels were calculated for strong fields. While the exact energy levels are given by the Breit-Rabi[51] formula, it suffices for all applications here to use the next term in its high field expansion. Accordingly, to the energies given by (164)–(167) must

[82] H. A. Bethe, Handbuch der Physik, second edition **24/1**, 386 (1933).
[83] A. G. Prodell and P. Kusch, Phys. Rev. **79**, 1009 (1950).

TABLE IV. Constants used for calculations of Zeeman and hyperfine splittings.

Quantity	Hydrogen	Deuterium
f_1 (Mc/sec)	7311.642	7313.631
H_1 (gauss)	5217.801	5219.220
H_{1a} (gauss)	5222.208	5222.919
H_1 (gauss)	5209.008	5211.840
T	−0.0033703	−0.0028284
Δw (Mc/sec)	177.551	40.923

be added

$$w=\Delta w(I+\tfrac{1}{2})^{-1}m_I m_S-g_I\mu_0 H m_I + (\Delta w)^2(I+\tfrac{1}{2})^{-2}(2g_S\mu_0 H)^{-1} \times[\{I(I+1)-m_I^2\}m_S-\tfrac{1}{2}m_I]. \quad (175)$$

The last term may be written as

$$C(m_S, I, m_I)(\Delta w/g_S\mu_0 H)\Delta w \quad (176)$$

where the coefficients $C(m_S, I, m_S)$ are given in Table V.

(b) P States

For p states, the interaction (173) may be simplified to

$$w_{11}=g_I\mu_0^2(r^{-3})_{Av}[2\mathbf{I}\cdot\mathbf{L}+\tfrac{1}{5}g_S\{4\mathbf{I}\cdot\mathbf{S}-3\mathbf{I}\cdot\mathbf{L}\mathbf{L}\cdot\mathbf{S} -3\mathbf{L}\cdot\mathbf{S}\mathbf{I}\cdot\mathbf{L}\}] \quad (177)$$

with neglect of some terms of relative order α^2. This operator has matrix elements diagonal in $\mathbf{J}$ which can be written in the form (53) if the small difference between g_S and 2 is neglected (see Appendix VI) or as

$$(J|w_{11}|J)=\Delta w(\mathbf{I}\cdot\mathbf{J})/[2(2I+1)J(J+1)] \quad (178)$$

in terms of the hyperfine separation Δw for $2^2S_{\frac{1}{2}}$. In case of good Russell-Saunders coupling, the hyperfine splitting would be just as given by (53) or in the Back-Goudsmit limit

$$w=\tfrac{1}{4}[\Delta w/((I+\tfrac{1}{2})J(J+1))]m_I m_J. \quad (178a)$$

Since the experiments are conducted in an appreciable magnetic field, the vectors $\mathbf{L}$ and $\mathbf{S}$ are somewhat decoupled, and a correction must be applied in Eq. (178a). The elements of w_{11} off-diagonal in $\mathbf{J}$ may be written in the form

$$(J'|w_{11}|J)=\tfrac{1}{16}\Delta w(I+\tfrac{1}{2})^{-1}(J'|\mathbf{I}\cdot\mathbf{L}|J) \quad (179)$$

TABLE V. Values of coefficients $C(m_S, I, m_I)$ of Eq. (176).

		α	β
$I=\frac{1}{2}$	$m_I=\frac{1}{2}$	0	−1/4
	$m_I=-\frac{1}{2}$	1/4	0
$I=1$	$m_I=1$	0	−2/9
	$m_I=0$	2/9	−2/9
	$m_I=-1$	2/9	0

and the necessary matrix elements of $\mathbf{I}\cdot\mathbf{L}$ calculated from equations given by Condon and Shortley.[84]

The complete effective Hamiltonian for Zeeman and hyperfine energy of the $2p$ states is then

$$\mathcal{H}=\Delta E\delta_{J\frac{1}{2}}+\mu_0\mathbf{H}\cdot(g_S\mathbf{S}+g_L\mathbf{L})+w_{11}-g_I\mu_0\mathbf{H}\cdot\mathbf{I}. \quad (180)$$

In the n, J, m_J, m_I representation only the first and last terms in $\mathcal{H}$ are diagonal. If the last two terms were neglected and perturbation theory correct to all orders in $\mu_0 H/\Delta E$ were applied to the second term in (180), the result would be equivalent to a power series expansion in x of Eqs. (164–(167)). It is convenient to take the diagonal elements in J of the second term, namely

$$g_J\mu_0\mathbf{H}\cdot\mathbf{J} \quad (181)$$

where g_J is the Landé factor for state J, as part of the unperturbed Hamiltonian. The application of perturbation theory to the remainder of $\mathcal{H}$ then gives the above power series expansion as well as some new contributions arising from cross products of the second and third terms as well as powers of the third term. These contributions are of order

$$(\Delta w)^2/\mu_0 H, \quad \Delta w\mu_0 H/\Delta E, \quad (\Delta w)^2/\Delta E$$

etc., and from a rough estimate of their magnitude it is clear that only the first two need be retained for the analysis of the present experiments.

The cross-product term from second-order perturbation theory for $2^2P_{\frac{1}{2}}$ and $2^2P_{\frac{3}{2}}$ respectively may be written as

$$\pm(2/9)[g_J g_I\mu_0^2(r^{-3})_{Av}/\Delta E]\mu_0 H m_I \quad (182)$$

or in terms of the hyperfine splitting Δw for $2^2S_{\frac{1}{2}}$ as

$$\pm(1/36)(\Delta w/\Delta E)(I+\tfrac{1}{2})^{-1}\mu_0 H m_I. \quad (183)$$

This can be regarded as equivalent to a change in the nuclear g-value from g_I to

$$g_I'=g_I\mp(1/36)(\Delta w/\Delta E)(I+\tfrac{1}{2})^{-1}$$

as far as the energy of orientation in a magnetic field is concerned.

If it were not for this correction to g_I for p-states, the nuclear magnetic orientation energy

$$-g_I\mu_0 H m_I$$

could be ignored completely, because m_I does not change in the allowed transitions. Because of the change in effective g_I for p-states, however, there is a slight change in the separation of the resonance peaks amounting to an increase of

$$(1/18)[I/(I+\tfrac{1}{2})](\Delta w/\Delta E)\mu_0 H$$

or 0.63 and 0.19 Mc/sec/kilogauss for hydrogen and deuterium, respectively, in the case of transitions αa, αb, αc, and a decrease by the same amount for αe and αf.

[84] Condon and Shortley, *Theory of Atomic Spectra* (Cambridge University Press, London, 1935), p. 64.

This will make itself felt primarily in the observed width of a composite resonance curve and the degree of resolution of the constituent peaks for the various m_I values, but not in the apparent center of the composite curve.

The term of order

$$(\Delta w)^2/\mu_0 H$$

corresponds to the expansion for high magnetic field of the hyperfine energy given by the Breit-Rabi formula, and in fact is more general, since it applies for p states when neither I nor J is $\frac{1}{2}$. It is

$$(1/64)[\Delta w/(I+\tfrac{1}{2})]^2[J(J+1)]^{-2}(g_J\mu_0 H)^{-1} \cdot[m_J\{I(I+1)-m_I^2\}-m_I\{J(J+1)-m_J^2\}]. \quad (184)$$

57. Stark Effect

The presence of an electric field in the rf interaction space gives rise to displacements of the fine structure energy levels. Except for cases of near degeneracy such as occur in study of the $\alpha\beta$ transitions at 575 gauss for magnetic field calibration and treated in Chapter N, it suffices to use second-order perturbation theory to calculate the Stark shift of a level i

$$\Delta W_i=-\sum_n|(n|e\mathbf{E}\cdot\mathbf{r}|i)|^2/(E_n-E_i). \quad (185)$$

Assuming Russell-Saunders coupling, the matrix elements of x, y, and z in units of the Bohr radius a_0 are given in Table VI for the various transitions Although at the actually used magnetic fields, there is some departure from Russell-Saunders coupling, the Stark perturbation is small and the above matrix elements are sufficiently accurate. In addition, the denominator in Eq. (185) may be evaluated assuming a nominal level shift of 1060 Mc/sec, and a magnetic splitting given in weak field approximation by

$$g_J^{(0)}\mu_0 H m_J \quad (186)$$

using the usual Landé g-values (142a), and neglecting hyperfine splitting.

Taking only the motional electric field

$$E_y=VH/c \quad (187)$$

into account, one finds

$$|(n|e\mathbf{E}\cdot\mathbf{r}|i)|^2=e^2H^2(V^2/c^2)_{\text{Av}}|(n|y|i)|^2. \quad (188)$$

The average shift depends on $(V^2)_{\text{Av}}$ for the beam, and assuming the distribution (88)

$$V^2=(V^2)_{\text{Av}}=2U^2=2(2kT/M) \quad (189)$$

where M is the atomic mass. For an oven temperature of 2500°K, and a magnetic field $H=1159$ gauss (transition αe at 2195 Mc/sec), one finds

$$(E_y)_{\text{rms}}=VH/c=10.5 \text{ volt/cm}, \quad (190)$$

TABLE VI. Values of matrix elements of coordinates for various transitions in weak magnetic field.

Transitions		x	y	z
αa	βd	$3/\sqrt{2}$	$\pm 3i/\sqrt{2}$	0
αb	βc	0	0	$\sqrt{6}$
αc	βb	$\sqrt{3}/\sqrt{2}$	$\mp i\sqrt{3}/\sqrt{2}$	0
αd	βa	0	0	0
αe	βf	0	0	$\pm\sqrt{3}$
αf	βe	$\sqrt{3}$	$\pm i\sqrt{3}$	0

and

$$eVHa_0/hc=13.47 \text{ Mc/sec} \quad (191)$$

for hydrogen, and $1/2^{\frac{1}{2}}$ as much for deuterium.

When the Stark effect shifts are small, one may neglect any asymmetries produced by them, and merely calculate their magnitude at the center of the observed resonance curve. Thus for state α of hydrogen at 1159 gauss the contributions from states a, c, and f to (185) are -0.07, -0.04, and 0.17 Mc/sec, respectively, so that state is raised by 0.06 Mc/sec. On the other hand, state e is more strongly repelled by the nearby state β and raised by an amount 0.52 Mc/sec. Accordingly the frequency for αe is lowered by 0.46 Mc/sec, which implies an increase by 0.46 Mc/sec in the level shift as calculated from the data for hydrogen without Stark effect, and by half that amount for deuterium. Similarly, there are corrections of -0.13 and -0.06 Mc/sec to be applied to results obtained from transition αf at 2395 Mc/sec. Such corrections will be applied in Part IV in the analysis of the data.

There is also an error in magnetic field calibration using transition $\alpha\beta$ at 575 gauss. Presumably, the Stark shift of state β by the degenerate level e is very small as indicated in Sec. (72), but there are shifts due to distant levels. For deuterium, these increase the frequency of $\alpha\beta$ by 0.032 Mc/sec, and therefore all magnetic fields should be lowered by a negligible fractional amount 0.032/((2.803)(5751)) or 0.02 percent.

There is evidence, discussed in Part IV, that electric fields amounting to as much as one volt per centimeter due to contact potentials or charged insulating films may be present in the interaction space. It can be seen from the above estimates that such fields would produce a wholly negligible Stark effect. The possibility of shifts produced by the rf fields used for the measurements will be discussed in Sec. 66.

58. Summary

The formulas and constants necessary for energy level calculations to the required accuracy have been given in Secs. 53–57, especially in Tables II, IV, and V and Eqs. (135), (136), (164)–(172), (175), (176), (178a), (182)–(185). A few additional effects are studied in Appendix VI, but, except for an additive contribution to δ from the finite size of the deuteron, they are numerically negligible.

L. RADIATIVE CORRECTIONS TO RESONANCE LINE FORM

59. Ideal Weisskopf-Wigner Line Form

The goal of the Weisskopf-Wigner[85] theory of radiation broadening was to obtain the basic form of resonance curve

$$\mu \propto [(\nu-\omega)^2+\tfrac{1}{4}\gamma^2]^{-1} \qquad (192)$$

where ν is the circular frequency of the radiation (rf in this case), ω the frequency of the transition, and γ is the reciprocal life time of the decaying $2p$ state. It may be recalled that in the original Weisskopf-Wigner theory, there appeared a divergent integral which had to be discarded in order to obtain Eq. (192) without an infinite shift in the resonance frequency. Serpe[86] showed that this divergent integral could be interpreted as a part of the self-energy due to the interaction of the electron with the radiation field. Presumably with the more powerful theoretical techniques[87] now available for handling divergent field theories, the problem of radiative line shape could be treated in a satisfactory way: the infinite terms would disappear and the finite level shifts of Bethe[73,75] would properly appear in the denominator. Unfortunately this does not appear to have been done as yet, but there is little doubt that a result much like Eq. (192) would be obtained for the basic resonance shape. It might be mentioned that a shift of resonance frequency such as that associated with the damping of a classical harmonic oscillator, of order $\gamma^2/\omega(2p\rightarrow 1s)$, is completely negligible for the $2p$ state of hydrogen.

60. Possible Corrections to Weisskopf-Wigner Line Form

It is still possible that (192) should be modified in some way. For instance, there might be added an antiresonant term

$$[(\nu+\omega)^2+\tfrac{1}{4}\gamma^2]^{-1}. \qquad (193)$$

Indeed, such a contribution appears in some derivations, but for $\nu/2\pi\sim\omega/2\pi\sim 2400$ Mc/sec, it is 9200 times smaller than the resonant term, and is completely negligible for the present discussion.

When the derivation of Appendix II is repeated with $\mathbf{E}$ replaced by $\mathbf{E}\exp(-i\nu t)$, Eq. (76) becomes equivalent to (192). If, however, the perturbation is written in terms of a vector potential $\mathbf{A}$ of the rf field as $-(e/m)\mathbf{A}\cdot\mathbf{p}$ instead of $e\mathbf{E}\cdot\mathbf{r}$ an additional factor $(\omega/\nu)^2$ appears in (192). This would give rise to a significant distortion of the resonance curve, and it is therefore important to choose the correct form for analysis of the data. Of course, the difference between the perturbations $\mathbf{E}\cdot\mathbf{r}$ and $-(\mathbf{A}\cdot\mathbf{p})/m$ just corresponds to a gauge transformation under which the theory is known to be invariant, so that both perturbations must lead to the same physical predictions. Nevertheless, a closer examination shows that the usual interpretation[88] of probability amplitudes is valid only in the former gauge, and no additional factor $(\omega/\nu)^2$ actually occurs.

The Van Vleck-Weisskopf[89] formula for collision broadened lines does contain a factor involving ω/ν which has been confirmed[90] experimentally. There is, however, a fundamental difference between collision and radiative damping, so it should not be expected that the collision line shape would be obtained here.

61. Rf Power Shifts

Just as a shift of resonance frequency can be produced by a static electric field, it is possible for such a displacement to arise from an rf electric field, in particular, the rf field used to produce the observed quenching. A treatment of this problem is given in Appendix IV. The result is that no significant correction to the resonance position is needed for rf powers used in the precision experiments.

M. NONRADIATIVE CORRECTIONS TO LINE FORM

In Sec. 45 a number of causes for asymmetries and shifts of resonance peaks were listed. We now turn to a detailed consideration of such effects. The basic assumption is that under the influence of rf fields each metastable state decays at a rate γ given by Eq. (25). In case overlap of nearby peaks is deemed important, μ is taken as the sum of such terms. The observed beam consists of atoms with various velocities distributed among the various hyperfine components of states α and β. For the precision work, a magnetic field is chosen for which the β-contribution to the signal is at most only a few percent of that from α, so a separate correction for presence of atoms in the β-state can be made.

62. Effect of Saturation and Velocity Distribution

Of the metastable atoms in state (α, m_I) and having speed v a fraction

$$\phi=1-\exp[-\mu(m_I, H)l/v] \qquad (194)$$

is quenched while passing through an rf field of length l. This fraction must be averaged over hyperfine states and also over velocities of atoms in the beam. To a certain extent, the distribution of velocities is uncertain. Fortunately, as shown in Appendix V, the results are not appreciably dependent on this. For the calculations described below, the distribution (88) is used and gives a fractional quenching of a beam with initially un-

[85] V. F. Weisskopf and E. P. Wigner, Z. Physik **63**, 54 (1930) and **65**, 18 (1930).
[86] J. Serpe, Physica **7**, 133 (1940).
[87] See, for example, F. J. Dyson, Phys. Rev. **75**, 486 (1949).
[88] I am indebted to Professor L. H. Thomas for a helpful discussion of this point.
[89] J. H. Van Vleck and V. F. Weisskopf, Revs. Modern Phys. **17**, 227 (1945).
[90] G. Becker and S. Autler, Phys. Rev. **70**, 300 (1946).

polarized nuclear spins

$$\phi=[2U^{-4}/(2I+1)]\sum_{m_I=-I}^{I}\int_0^\infty[1-\exp\{-\mu(m_I,H)l/v\}]\times\exp(-v^2/U^2)v^3dv. \quad (195)$$

In terms of the function

$$G(\psi)=2\int_0^\infty[1-\exp-(\psi/z)]\exp(-z^2)z^3dz \quad (196)$$

which is plotted in Fig. 48 and whose properties are discussed in Appendix V, this becomes

$$\phi=[1/(2I+1)]\sum_{m_I=-I}^{I}G(\psi_m) \quad (197)$$

where

$$\psi_m=\mu(m,H)l/U. \quad (198)$$

As a starting point, we ignore overlap from other resonances and curvature of the Zeeman lines, and express the resonance parameters ψ_m in terms of frequency units ξ (megacycles per second) from their peaks

$$\psi_m=Ab^2/[(\xi-a_m)^2+b^2] \quad (199)$$

where A is proportional to the rf intensity, and $2b=\gamma$ gives the radiative width (99.692 Mc/sec for hydrogen and 99.719 Mc/sec for deuterium). The values of a_m depend on the hyperfine splitting of the initial and final states. In the approximations of Part I, for hydrogen, $a_{\frac{1}{2}}=-a_{-\frac{1}{2}}=58.5$ Mc/sec for αf and 29.3 Mc/sec for αe. Because of incomplete Back-Goudsmit effect, and other small corrections, the separations of the two peaks are slightly different, and improved values are used so that the spacing of the hyperfine peaks is theoretically correct. The shift of the center is taken into account subsequently together with the Zeeman curvature. For deuterium, in the above approximation $a_0=0$, $a_1=-a_{-1}=18$ Mc/sec for αf and half as much for αe.

The following procedure was adopted. All data for a given transition was taken with the rf power set to give a prescribed percentage of quenching at the center of the resonance. From the quenching at the center, it was then possible to determine the constant A of Eq. (199) independently of rf intensity, or values of $|(n|\mathbf{e}\cdot\mathbf{r}|\alpha)|^2$, l or U and to calculate the resonance curve for this value of A. When some factor leading to asymmetry or shift was to be considered, Eqs. (197)–(199) were modified accordingly, and the correction to the apparent center as measured at the prescribed level was determined. Since all considered effects led to very small shifts, it was sufficient to find such corrections independently and to add the results.

To illustrate these calculations, the case of transition αe in hydrogen at 2195 Mc/sec will be considered in detail, with results given as needed for other cases in Part IV. A panoramic view of the dependence on magnetic field of rf quenching at 2195 Mc/sec was given in Fig. 36. The peak quenching for αe was chosen arbitrarily as 31 percent, which was neither too small for accurate measurements or large enough to give serious saturation effects. As explained in Sec. 45, it was proposed to locate the center of each resonance by finding points on each side which gave equal quenching. These are called the "working points" and in the case chosen for illustration were taken at the 21 percent quenching level. It was possible to ignore the effect of overlap from the much weaker αf peak in this case.

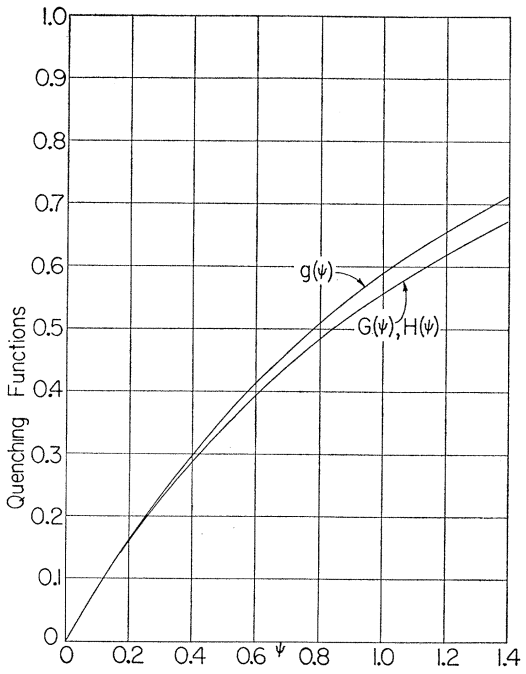

FIG. 48. Quenching functions for various assumed velocity distributions as dependent on a variable ψ which is proportional to the rate of transitions. The function $G(\psi)$ (defined in Eqs. (196) and (237)) applies for a thermal velocity distribution, while $g(\psi)$ (Eq. (241)) is obtained for an equivalent single velocity. When bombardment recoil is taken into account, there results a function $H(\psi)$ which is numerically hardly distinguishable from $G(\psi)$.

63. Variations of Matrix Element Across Resonance

The rate of decay of the metastable state α induced by rf depends on the squares of the matrix elements of $\mathbf{r}$ to the various p states. The values of these in weak magnetic field approximation are given in Table VI. At the fields used in the precision measurements, a departure from the weak field values is to be expected, and since the matrix element varies across the resonance curve because of the changing magnetic field, there is a significant amount of distortion which requires a correction.

Bethe[91] has given the intermediate field wave functions from which the matrix elements of $\mathbf{r}$ may be

[91] See reference 82, p. 398.

calculated. The results may be expressed in terms of correction factors $C(\alpha n)$ to the squared matrix elements $|(n|\mathbf{r}|\alpha)|^2$ evaluated in weak field. These are

$$\begin{aligned} C(\alpha a)&=1,\\ C(\alpha b)&=\tfrac{3}{4}(1+\delta_+),\\ C(\alpha c)&=\tfrac{3}{2}(1+\delta_-),\\ C(\alpha e)&=\tfrac{3}{2}(1-\delta_+),\\ C(\alpha f)&=\tfrac{3}{4}(1-\delta_-), \end{aligned} \tag{200}$$

where

$$\delta_\pm=(\pm\tfrac{1}{2}+x)[(9/4)\pm x+x^2]^{-\frac{1}{2}} \tag{201}$$

using the dimensionless magnetic field unit of Eq. (172). With these correction factors inserted into Eq. (199), the constant A was readjusted to bring the quenching at the center back to the standard value, and the error in the apparent center at the working point level determined. For the case of transition αe in hydrogen at 2195 Ms/sec, a correction of -0.58 Mc/sec to the apparent level shift is required.

64. Quenching Asymmetry

The preceding discussion assumed that the beam was composed of atoms divided equally among the $(2I+1)$ hyperfine states (α, m_I). If electric fields are present, these states are differently quenched because of different energy separations from competing p states. This gives rise to an asymmetry and shift of the resonance curves. The most important cause of quenching is presumably the motional electric field, and only this was taken into account in the following discussion.

The decay rate due to motional Stark effect is given as a sum of terms like (42) for transitions from α to states a, c, and f. Ignoring the slight differences in the dimensionless magnetic field variables x for the various states, the decay rate may be written as

$$\begin{aligned}\lambda=\gamma(ea_0/\mu_0)^2(V/c)^2x^2\cdot[&(9/2)(y_{a\alpha}{}^2+\tfrac{1}{4}\Gamma^2)^{-1}\\ &+(3/2)(y_{c\alpha}{}^2+\tfrac{1}{4}\Gamma^2)^{-1}+3(y_{\alpha f}{}^2+\tfrac{1}{4}\Gamma^2)^{-1}],\end{aligned} \tag{202}$$

where γ is the decay rate of $2p$, a_0 the Bohr radius, μ_0 the Bohr magneton, V the speed of the atom at right angles to the magnetic field, x is the magnetic field measured in units of 5214 gauss, while the dimensionless damping constant Γ has the value $100/7300=0.0151$. The energy separations are proportional to $y_{a\alpha}=y_a=y_\alpha$, etc. and are supposed to include hyperfine splittings as well as an (approximate) value for the S level shift. In the cases of interest, however, the decay is induced mostly by state f, so that hyperfine splitting need be taken into account only in the third term. As indicated in Fig. 17, for hydrogen $y_{\alpha f}$ is increased by 58.5/7300 for $m_I=\frac{1}{2}$, and decreased by the same amount for $m_I=-\frac{1}{2}$.

Since the rate of decay due to motional electric field varies with the square of the atomic speed V, and the time spent in travelling a distance l from electron bombarder to detector varies inversely with V, only a fraction $\exp-\lambda l/V$ of the excited atoms will reach the detector in the absence of rf fields, where $\lambda l/V$ is proportional to V. The fractional quenching produced by rf may then be written as

$$\phi=\textstyle\sum_m G(\psi_m,\rho_m)/\sum_m G(\infty,\rho_m) \tag{203}$$

where

$$G(\psi,\rho)=2\int_0^\infty e^{-\rho y}(1-e^{-\psi/y})e^{-y^2}y^3dy \tag{204}$$

with ψ_m given by Eq. (198), and

$$\rho_m=\lambda^{(0)}{}_m l/U \tag{205}$$

where $\lambda^{(0)}$ is the value of λ for $V=U$, the velocity used in Eq. (88). The integral $G(\psi,\rho)$ may be evaluated by expanding $\exp-\rho y$ in a power series in ρy and integrating term by term. The first integral is just the tabulated $G(\psi)$. The subsequent integrals may be expanded in powers of ψ and integrated term by term with sufficient approximation. The values of ϕ calculated at the working points $\xi=\pm 58.8$ Mc/sec for the case at hand are 21.528 percent and 21.478 percent, respectively, and after conversion into a correction to the apparent center of the resonance curve, imply a decrease of the level shift by 0.08 Mc/sec.

65. Incomplete Back-Goudsmit Effect and Nonlinear Zeeman Splitting

At the magnetic fields used in the experiments, the nuclear spin is not fully decoupled from the other angular momenta of the atom. As a result, the hyperfine levels are unsymmetrically distributed about the energy obtained without hyperfine structure. The apparent center of the composite resonance curve is accordingly displaced from the position it would have in the absence of hyperfine structure. The correction to the level shift can be obtained by using unequal values for the a_m in Eq. (199) and calculating the apparent center. (The case of hydrogen with two component peaks could be treated more simply.)

The resonance curves are taken with fixed radio frequency by varying the magnetic field. Due to nonlinear dependence of the Zeeman splitting on magnetic field caused by progressive decoupling of $\mathbf{L}$ and $\mathbf{S}$ a distortion of the resonance arises. Letting h be the distance in gauss measured from the true center of a resonance curve, one may write with sufficient approximation in Eq. (199).

$$\xi\rightarrow\xi_m=c_mh+d_mh^2 \tag{206}$$

where c_m are the slopes of the frequency *versus* magnetic field curves for hyperfine component m, evaluated at the corresponding resonance field. In the calculations based on the ideal resonance curve this slope was evaluated at the center of the composite curve, while the curvature represented by d_mh^2 and asymmetry represented by unequal a_m were neglected. The com-

posite resonance curve was then calculated as a function of h, and the departure of the apparent center from $h=0$ was determined. For the case being illustrated, corrections of -0.81 Mc/sec and -0.11 Mc/sec, respectively, must be applied to the apparent level shift because of the incomplete Back-Goudsmit effect and the Zeeman curvature.

66. Correction for Rf Power Variation

A correction must be applied for rf power variation, both because of slow changes in oscillator output during a run, and also to bring the peak quenching exactly to the prescribed value. An approximate basis for such a correction was indicated in Eq. (102) on the assumption of a linear relationship between rf intensity and I_x and that ϕ is proportional to power. The former assumption is valid for the limited range of I_x values occurring in a run, but the second requires small ϕ. In order to test this point, $(d\phi/dA)/(d\phi/dA)_0$ was calculated for the case under study ($\phi_0=31$ percent), and found to be sufficiently near to ϕ/ϕ_0 that Eq. (102) could be used.

67. Effect of Radiation from Quenched Atoms

As described in Sec. 42, there is a background signal due to ultraviolet radiation produced in the bombardment region. Except for fluctuations the effect of this is eliminated when the ratio of rf to dc quenching is computed. In addition, there is a detector signal produced by the Lyman L_α radiation emitted in the interaction region when the metastable atoms are quenched by rf and dc fields. Fortunately this introduces no error in the fractional quenching. To see this, let η and η' be efficiencies of detection of metastable atoms and photons, respectively, and let Ω be the average solid angle subtended by the detector from the quenching region. Then if the magnitude of the unquenched beam signal is denoted by ηB, the signal received when a fraction ϕ of the metastables is quenched is

$$\eta B(1-\phi)+\eta' B\phi(\Omega/4\pi)$$

and the apparent fraction quenched is

$$\phi_{\text{app}}=\frac{\text{rf quenching}}{\text{dc quenching}}=\frac{\eta B\phi-\eta' B\phi(\Omega/4\pi)}{\eta B-\eta' B(\Omega/4\pi)}=\phi$$

so that no error results from the photons produced in the measurement of ϕ, although the dc and rf quenching are separately reduced. If one used values $\eta=0.4$ and $\eta'=0.08$ such as found by Dorrestein[92] for helium, the corrections to these would also be small since $\Omega/4\pi \sim 0.02$. If in fact η were much smaller relative to η' the apparent signal would be reduced (or even reversed in sign!). All indications are that $\eta \gg \eta'(\Omega/4\pi)$, although from the signal size it was concluded in Sec. 26 that η was probably much less than 0.4. (Observations in which large voltages of either sign are applied across the detector are compatible with the relation $\eta \sim \eta'$ but a more accurate study should be made.)

[92] R. Dorrestein, Physica **9**, 433 and 447 (1942).

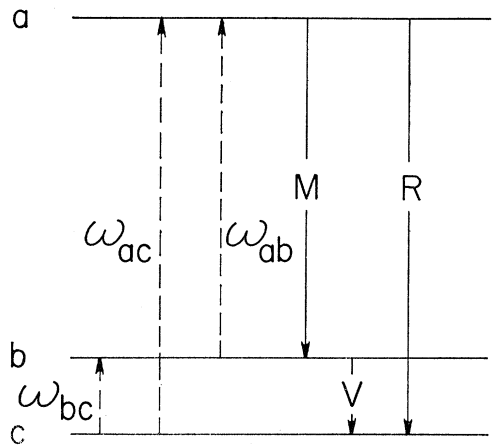

FIG. 49. Energy levels involved in sharp resonances $\alpha\beta$. Letters a and b represent states α and β ($2^2S_{\frac{1}{2}}$, $m_s=\frac{1}{2}$ and $-\frac{1}{2}$, respectively), while c represents state e ($2^2P_{\frac{1}{2}}$, $m_j=\frac{1}{2}$) which crosses β for $H=575$ gauss. The circular frequency separations ω_{ac}, etc. are shown and the perturbing matrix elements connecting various states: $\hbar R$ for electric dipole and $\hbar M$ for magnetic dipole energies due to rf fields, and $\hbar V$ the perturbing energy due to motional electric field.

N. THEORY OF $\alpha\beta$ TRANSITIONS

68. Statement of Problem

As explained in Sec. 44, it is possible to induce transitions from state α to state β which are much sharper than the transitions to nonmetastable states. These narrow resonances have been used to calibrate the magnetic field (Sec. 39), but since their appearance is rather unusual, it is necessary to have a theory of their shape in order to allow for any asymmetry shifting the apparent center.

Magnetic dipole transitions from α to β may occur because of the interaction $g_S\mu_0\mathbf{S}\cdot\mathbf{H}$ of the magnetic moment of the electron with a component of the rf magnetic field at right angles to the static magnetic field. It is also possible for electric dipole transitions to occur because the state β contains some p state contamination due to the motional electric field $\mathbf{E}=(V/c)\times\mathbf{H}$. In practice, the second mechanism is usually more important than the first.

69. Wave Equations

We consider three states $\alpha(2^2S_{\frac{1}{2}}, m_s=\frac{1}{2})$, $\beta(2^2S_{\frac{1}{2}}, m_s=-\frac{1}{2})$, and $e(2^2P_{\frac{1}{2}}, m_j=\frac{1}{2})$, as in Fig. 49, denoting their probability amplitudes by letters a, b, and c, respectively. The equations of time dependent perturbation theory are then

$$\begin{aligned} i\dot{a}&=\tfrac{1}{2}M^*b\exp[i(\omega_{ab}-\nu)t]+\tfrac{1}{2}R^*c\exp[i(\omega_{ac}-\nu)t],\\ i\dot{b}&=\tfrac{1}{2}Ma\exp[-i(\omega_{ab}-\nu)t]+V^*c\exp(i\omega_{bc}t),\\ i\dot{c}&=\tfrac{1}{2}Ra\exp[-i(\omega_{ac}-\nu)t]+Vb\exp(-i\omega_{bc}t)-\tfrac{1}{2}i\gamma c. \end{aligned} \tag{207}$$

The circular frequency separation of state a from b is, denoted by ω_{ab} while ν is the circular radiofrequency.

As in Appendix II of Part I only the perturbation terms capable of resonance are considered. Equations (207) imply that states b and c are coupled by a perturbation with matrix element V of the motional electric field energy $e(\mathbf{V}/c)\times\mathbf{H}\cdot\mathbf{r}$, while because of the presence of radio waves magnetic dipole transitions between a and b occur with a matrix element M and electric dipole transitions between a and b occur with a matrix element R. Only the p state e is coupled by radiation to the ground state $1^2S_{\frac{1}{2}}$, and this is allowed for phenomenologically by introduction of a decay constant $\gamma=1/\tau_p$ as in Appendix II.

70. Solution of Wave Equation

The wave equations (207) have a general solution of the form

$$\begin{aligned} a&=\sum_{k=1}^{3} A_k \exp(-\mu_k t),\\ b&=\sum_{k=1}^{3} B_k \exp[i(\nu-\omega_{ab})t-\mu_k t], \qquad (208)\\ c&=\sum_{k=1}^{3} C_k \exp[i(\nu-\omega_{ac})t-\mu_k t], \end{aligned}$$

where the μ_k are roots of a cubic equation

$$\begin{vmatrix} i\mu & \frac{1}{2}M^* & \frac{1}{2}R^* \\ \frac{1}{2}M & i\mu+\nu-\omega_{ab} & V^* \\ \frac{1}{2}R & V & i\mu+\nu-\omega_{ac}-\frac{1}{2}i\gamma \end{vmatrix}=0. \qquad (209)$$

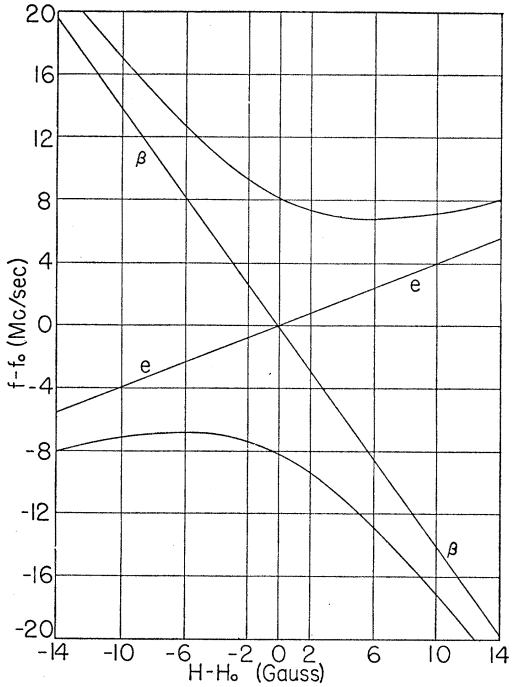

FIG. 50. Stark splitting of levels β and e as a function of magnetic field separation from the crossing field of 575 gauss. The straight lines indicate unperturbed energies and the curves show expected level splitting due to motional electric field according to usual degenerate perturbation theory.

The coefficients B_k and C_k are expressible in terms of the A_k by the equations

$$\begin{aligned} B_k&=-\tfrac{1}{2}A_k[M(\nu-\omega_{ac}+i\mu_k-\tfrac{1}{2}i\gamma)+RV^*]/\mathfrak{D}_k,\\ C_k&=-\tfrac{1}{2}A_k[R(\nu-\omega_{ab}+i\mu_k)+MV]/\mathfrak{D}_k, \end{aligned} \qquad (210)$$

where

$$\mathfrak{D}_k=(\nu-\omega_{ac}+i\mu_k-\tfrac{1}{2}i\gamma)(\nu-\omega_{ab}+i\mu_k)-|V|^2.$$

The initial conditions $a=1$, $b=c=0$ at $t=0$ require

$$\sum_{k=1}^{3} A_k=1, \quad \sum_{k=1}^{3} B_k=0, \quad \sum_{k=1}^{3} C_k=0 \qquad (211)$$

and these equations suffice to determine the A_k.

71. Discussion of Roots. Violation of "No-Crossing" Theorem

In practice, the roots μ_1, μ_2, μ_3 differ greatly from one another in the values of

$$\mu_k+\mu_k^*.$$

The largest of these, $\mu_1+\mu_1^*$, corresponds closely to the radiative decay rate γ of the nonmetastable state e, the intermediate value

$$\mu_2+\mu_2^*$$

is related to the Stark induced rate of decay of the lower $2^2S_{\frac{1}{2}}$ state β, while $\mu_3+\mu_3^*$ essentially determines the decay rate of the upper $2^2S_{\frac{1}{2}}$ state α caused by radio waves. If R and M are neglected, the two larger roots are solutions of the quadratic equation

$$\mathfrak{D}(\mu)\equiv\begin{vmatrix} i\mu-(\omega_{ab}-\nu) & V^* \\ V & i\mu-(\omega_{ac}-\nu+\frac{1}{2}i\gamma) \end{vmatrix}=0. \qquad (212)$$

If the damping term $\frac{1}{2}i\gamma$ were absent, this would be equivalent to the secular equation for determination of the static Stark effect splitting of the approximately degenerate levels β and e. When the perturbation $|V|$ is large compared to $|\omega_{bc}|$ the splitting is linear in $|V|$ while it is quadratic in $|V|$ for $|V|\ll|\omega_{bc}|$. The presence of a damping term γ, however, essentially modifies the nature of the Stark effect when $\gamma\gtrsim 4|V|$. The two roots for small $|V|$ are then approximately

$$\begin{aligned} i\mu_1&\sim\tfrac{1}{2}i\gamma+(\omega_{ac}-\nu)+|V|^2/(\omega_{bc}+\tfrac{1}{2}i\gamma)\\ i\mu_2&\sim(\omega_{ab}-\nu)-|V|^2/(\omega_{bc}+\tfrac{1}{2}i\gamma). \end{aligned} \qquad (213)$$

The real part of the second root is given by

$$\mu_2+\mu_3^*=\gamma|V|^2/[\omega_{bc}^2+\tfrac{1}{4}\gamma^2] \qquad (214)$$

which is just the decay rate of the lower metastable state as calculated in Appendix II. The imaginary part

$$\tfrac{1}{2}i(\mu_2^*-\mu_2)=\omega_{ab}-\nu+\omega_{bc}|V|^2/[\omega_{bc}^2+\tfrac{1}{4}\gamma^2] \qquad (215)$$

implies a shift in the position of that state. When $|\omega_{bc}|\gg\frac{1}{2}\gamma$ the shift is just that to be expected for the quadratic Stark effect, but the shift is much reduced

for $|\omega_{bc}|<\frac{1}{2}\gamma$, and in fact, even vanishes for $\omega_{bc}=0$. This behavior is illustrated in Fig. 50 giving the energies of levels β and e as functions of magnetic field in the vicinity of their crossing point. In one case the electric field is zero and there is no coupling V between the states, while in the other, the usual phenomenon of energy level repulsion required by the famous von Neumann-Wigner[93] "no-crossing" theorem is shown for an electric field experienced by a 2500°K deuterium atom moving perpendicular to a magnetic field of 575 gauss. In Fig. 51 the change brought about by the radiative broadening of state e is indicated. The six solid curves correspond to six assumed values of the damping constant: (a) $\gamma=0$, (b) $\gamma=2V$, (c) $\gamma=(12)^{\frac{1}{2}}V$, (d) $\gamma=(15.36)^{\frac{1}{2}}V$, (e) $\gamma=4V\sim16$ Mc/sec (critical damping), and (f) the actual case $\gamma\sim100$ Mc/sec. The unperturbed levels are indicated by the dotted curves. It will be noted that for damping equal or above the critical value the "no-crossing" theorem is violated, and above critical damping the β-state largely retains its s character throughout. For subcritical damping, however, each level is a 50–50 mixture of s and p at the βe crossing point, and the life of each state is $2\tau_p$. The observation of sharp $\alpha\beta$ resonances at this magnetic field with a half-width of order 3 Mc/sec instead of 50 Mc/sec supports the theory of the reduced Stark splitting when one of the levels is highly damped. Such phenomena ought to occur in other problems of atomic and molecular physics, but could be observed only with instruments capable of exploring well within the radiative widths.

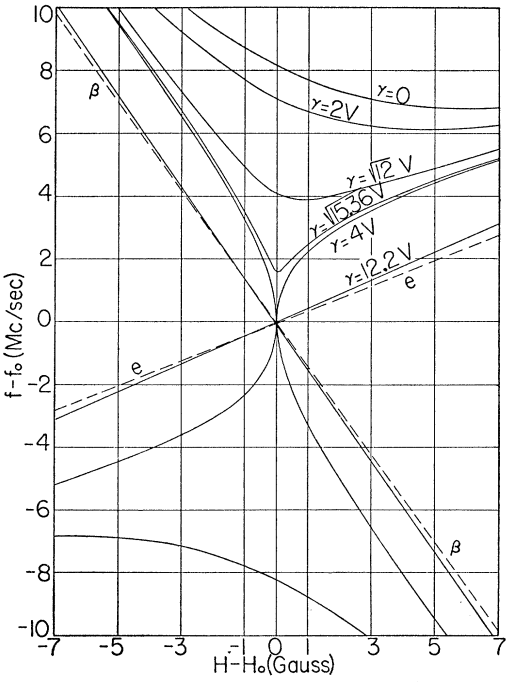

FIG. 51. Stark splitting of levels β and e as in Fig. 50 according to perturbation theory in which radiative decay of e is taken into account. Curves are shown for the motional electric field energy equal to its actual value with various assumed values for the damping constant γ. For $\gamma=0$, the curve of Fig. 50 is obtained. Critical damping occurs for $\gamma=4V$, while $\gamma=12.2V$ corresponds to the actual case with $\gamma/(2\pi)=100$ Mc/sec.

72. Calculation of Decay Constant

It will suffice, for present purposes, to calculate the small root μ_3 only to second order in R and M. One finds

$$i\mu_3=-\tfrac{1}{4}[|R|^2(\omega_{ab}-\nu)+MVR^*+M^*V^*R+|M|^2(\omega_{ac}-\nu+\tfrac{1}{2}i\gamma)]/\mathfrak{D}(0). \quad (216)$$

In the analysis of such a complicated expression, it is necessary to have a clear idea of orders of magnitude of all quantities entering the equation. The damping constant γ corresponds to a frequency of 100 Mc/sec, while the matrix element $V=(e/h)(v/c)H(e|y|\beta)$ for for deuterium at 575 gauss has a value corresponding to 8.2 Mc/sec.

If the rf field has approximately equal magnitudes of electric and magnetic fields, the matrix element R is much larger than M. In fact, $M/R\sim\mu_0/ea_0=\hbar/(2mca_0)=\frac{1}{2}\alpha\sim1/274$. Except for ν very near ω_{ab} the terms involving M in Eq. (216) may accordingly be neglected. Then

$$i\mu_3=-\tfrac{1}{4}|R|^2(\omega_{ab}-\nu)/[(\omega_{ab}-\nu)(\omega_{ac}-\nu+\tfrac{1}{2}i\gamma)-|V|^2]. \quad (217)$$

In the experiment, metastable atoms are formed in the bombardment region in both states α and β in equal numbers. After traversing a distance $L_1\sim3$ cm they enter the rf region of length $L_2\sim1$ cm and the survivors travel a further distance $L_3\sim2$ cm to the detector. For simplicity, we assume that state β has fully decayed before the atoms reach the rf region at time $t=0$. After passage through the rf region at time $t=L_2/V\sim1.2\times10^{-6}$ sec there will be a distribution of atoms in states $a=\alpha$, $b=\beta$, and $c=e$ with probabilities $|a|^2$, $|b|^2$, and $|c|^2$, respectively. The last state will strongly decay before the atoms strike the detector at a time later by $L_3/V\sim2.5\times10^{-6}$ sec. To obtain as much simplicity as possible, let us also assume that the same is true of atoms in state b. This assumption will be valid when the resonances are studied in the vicinity of the crossing point of β and e for then the decay rate $\mu_2+\mu_2^*$ is of order $\gamma/25$ as shown in Fig. 34. In the case of resonances $\alpha\beta$ studied at 2000 Mc/sec, state b is somewhat less well damped.

With these simplifications, the detector signal is proportional to

$$S\propto|A_3|^2\exp-(\mu_3+\mu_3^*)t. \quad (218)$$

The coefficient $|A_3|^2$ is less than unity (quenching of beam due to decay of transients), but is a slowly varying function of magnetic field in the vicinity of the sharp resonances so that we are more interested in the

[93] J. von Neumann and E. P. Wigner, Physik. Z. 30, 467 (1929).

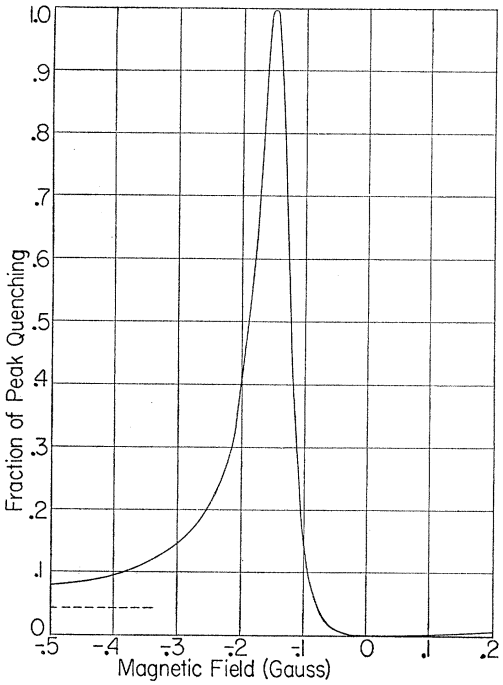

FIG. 52. Form of $\alpha\beta$ resonance expected from Eq. (219) at a frequency of 1995 Mc/sec. The fractional quenching is plotted against $H-H_0$.

rf induced decay rate given by

$$\mu_3+\mu_3^*=\tfrac{1}{4}\gamma|R|^2(\omega_{ab}-\nu)^2/ [\{(\omega_{ab}-\nu)(\omega_{ac}-\nu)-|V|^2\}^2+\tfrac{1}{4}\gamma^2(\omega_{ab}-\nu)^2]. \quad (219)$$

When $|\omega_{ab}-\nu|$ is large, and $|V|$ is sufficiently small, Eq. (219) simplifies to

$$\mu_3+\mu_3^*\rightarrow\tfrac{1}{4}\gamma|R|^2/[(\omega_{ac}-\nu)^2+\tfrac{1}{4}\gamma^2] \quad (220)$$

which is just the rate of rf induced transitions from α to e when only these two levels are present. The maximum decay rate is $|R|^2/\gamma$.

More generally, expression (219) vanishes when $\omega_{ab}-\nu=0$ and reaches a value (nearly a maximum) of $|R|^2/\gamma$ for the frequencies for which the first term in the denominator vanishes. For small $|V|$, these frequencies are near $\nu=\omega_{ac}$ for which Eq. (220) has its maximum, and $\nu=\omega_{ab}$ for which Eq. (219) has its zero.

The appearance of the resulting resonance curve (219) is quite different depending on whether $|\omega_{bc}|\gg\frac{1}{2}\gamma$ or $|\omega_{bc}|\ll\frac{1}{2}\gamma$. In the former case the resonance curve might appear as shown in Fig. 52. The resonance peak is displaced from the zero at $\nu=\omega_{ab}$ by an amount corresponding to the frequency $|V|^2/\omega_{bc}$, just the Stark shift of state b due to interaction with c. The curve is very similar to the experimental result of Fig. 42, but the observed width is much greater than that given by Eq. (219). The explanation of this discrepancy is that the transients of Eq. (208a) are not damped highly enough to justify their complete neglect in this case. In fact, it is necessary to take the transients into account to obtain a width of resonance compatible with the uncertainty principle. Although it is not difficult to write out the more complete solution, it would still be necessary to average it over the velocity distribution in the beam, since the position of the peak depends on velocity, and this would require considerable numerical integration. Consequently the observed peak could not be readily used for a highly precise magnetic field calibration, although the error would not be large if a rough correction for Stark effect were made.

The latter case, $|\omega_{bc}|\ll\frac{1}{2}\gamma$ offers more promise. In the vicinity of the crossing point $\omega_{bc}=0$, the damping given by Eq. (214) is more than adequate to permit neglect of terms containing μ_2. First expectations were that the $\alpha\beta$ resonances would be very broad in this region, and subject to a large Stark effect shift of order V from the unperturbed position. As indicated in Eq. (215), however, the radiative damping of state e greatly reduces the shift and quenching of the β-state. At the crossing point of the shifts of β and e actually vanish (except for small shifts due to distant levels). Plots of Eq. (219) as a function of magnetic field in the vicinity of the crossing point are given in Fig. 53. Since there is a distribution of velocities, the shape and half-width are affected, but the zero remains at $\nu=\omega_{ab}$. The curves are highly symmetrical, easy to observe, and afford a convenient method for calibration of magnetic field in terms of frequency. An example of a curve of this type, somewhat complicated by hyperfine structure was given in Fig. 43. It will be noted that the quenching at $\nu=\omega_{ab}$ does not fall to as low a value (about two-thirds of the peak for deuterium since one-third of the beam is in a given hyperfine state) as indicated by the preceding theory. While no quantitative comparison has been attempted with a more refined theory, it is believed that this discrepancy may be attributed to neglect of the coefficient $|A_3|^2$ in Eq. (218).

The reduction in transition probability which occurs when $\nu=\omega_{ab}$ was interpreted in Sec. 47 in terms of an equivalent electrical circuit Fig. 46. A more quantum-mechanical understanding of the phenomenon can be had from an examination of the third Eq. (207) which can be satisfied when $\nu=\omega_{ab}$ for $c=0$ and $dc/dt=0$ if a and b are related by $\frac{1}{2}Ra+Vb=0$. An examination of the solution reveals that after damping of transients this relation is satisfied, and the state oscillates between a and b with such phase and amplitude relations that the decaying state c is not excited.

The author has benefited from many helpful discussions with Professor N. M. Kroll.

APPENDIX IV. RADIOFREQUENCY POWER STARK EFFECT

The possibility of a shift in resonance frequency due to the presence of rf fields was mentioned in Sec. 60. Such shifts occur in the molecular beam radiofrequency resonance method as shown by Bloch and Siegert.[94] For a spin $S=\frac{1}{2}$ undergoing Larmor

[94] F. Bloch and A. Siegert, Phys. Rev. **57**, 522 (1940), also A. F. Stevenson, Phys. Rev. **58**, 1061 (1940).

precession in a magnetic field $H_0=\hbar\omega/g_s\mu_0$ and perturbed by a perpendicular oscillating rf magnetic field $H_1\cos\nu t$, they found an increase $\delta\omega$ in the resonance frequency of

$$\delta\omega=(\omega/16)(H_1/H_0)^2=(g_s\mu_0H_1)^2/(16\hbar(\hbar\omega)). \quad (221)$$

In the present case, the induced decay of $2^2S_{\frac{1}{2}}$ is described by Eqs. (68) with V taken in the form

$$V=\hbar R\cos\nu t \quad (222)$$

and for simplicity $\gamma_a=0$ and $\gamma_b=\gamma$

$$i\dot{a}=R^*e^{-i\omega t}(\cos\nu t)b, \quad (223a)$$

$$i\dot{b}=Re^{i\omega t}(\cos\nu t)a-\tfrac{1}{2}i\gamma b. \quad (223b)$$

If damping were neglected, the problem would be exactly that solved by Bloch and Siegert, but decay changes the character of the solution considerably. In practice, the atoms spend about a microsecond in the quenching fields, or many cycles of the rf and many half-lives of $2p$. Consequently a solution of (223) in terms of a rate of induced decay of state a is needed for practical analysis of the resonance experiments.

If the nonresonant parts of $\cos\nu t=\frac{1}{2}(e^{i\nu t}+e^{-i\nu t})$ were neglected, Eqs. (223) could be solved exactly, and with suitable approximations would lead to (192). As in the Bloch-Siegert treatment, the nonresonant parts of $\cos\nu t$ are responsible for a shift of resonance frequency.

We write

$$a=e^{-\mu t}+a_1(t) \quad (224)$$

where $\mu+\mu^*$ is the desired frequency dependent decay rate of $2^2S_{\frac{1}{2}}$, and the small $a_1(t)$ allows for departures from the simple exponential law. Equation (223b) is then solved with neglect of a_1 for b subject to the initial condition $b(0)=0$ giving

$$b=-\tfrac{1}{2}R[B_1\{e^{i(\omega-\nu)t-\mu t}-e^{-\frac{1}{2}\gamma t}\}+B_2\{e^{i(\nu+\omega)t}-e^{-\frac{1}{2}\gamma t}\}] \quad (225)$$

where

$$B_1=(\omega-\nu-\tfrac{1}{2}i\gamma+i\mu)^{-1} \quad \text{and} \quad B_2=(\omega+\nu-\tfrac{1}{2}i\gamma+i\mu)^{-1}.$$

When this result is inserted in (223a), one may equate slowly and rapidly varying terms separately to zero, obtaining

$$-i\mu=-\tfrac{1}{4}|R|^2(B_1+B_2) \quad (226)$$

and

$$i\dot{a}_1=-\tfrac{1}{4}|R|^2\cdot[B_1e^{2i\nu t}+B_2e^{-2i\nu t}-(B_1+B_2)(e^{-\frac{1}{2}\gamma t}+e^{-\frac{1}{2}\gamma t+2i\nu t})] \quad (227)$$

whose solution subject to $a_1(0)=0$ is

$$a_1=(i/4)|R|^2[B_1(e^{2i\nu t}-1)/(2i\nu)-B_2(e^{-2i\nu t}-1)/(2i\nu)+(B_1+B_2)\{(1-e^{-\frac{1}{2}\gamma t})/(\tfrac{1}{2}\gamma)+(1-e^{-\frac{1}{2}\gamma t+2i\nu t})/(\tfrac{1}{2}\gamma-2i\nu)\}]. \quad (228)$$

The first two terms represent a rapidly oscillating contribution to a_1 of amplitude at most of order

$$B_1|R|^2/8\nu\sim|R|^2/(4\gamma\nu) \quad (229)$$

which will be seen from the subsequent numerical discussion to be negligible for the rf power used in the precision experiments. The remaining terms vanish at $t=0$, but after $t=1/\gamma$ very rapidly take on a constant value. Besides the "secular" damping $1-\exp-(\mu+\mu^*)t$, there is according a "shock" damping which for $(\mu+\mu^*)t\ll1\ll\gamma t$ is approximately

$$-(a_1+a_1^*)\to\tfrac{1}{2}|R|^2(B_1+B_1^*)/\gamma\simeq\tfrac{1}{2}|R|^2/[(\omega-\nu)^2+\tfrac{1}{4}\gamma^2] \quad (230)$$

and is small compared to the secular term by a factor $2/(\gamma t)$ or about 1/400 in practice, and in any case leads to no asymmetry. It can also be easily verified that no significant error was made by neglecting a_1 in Eq. (223b) as long as

$$|R|^2/\gamma^2\ll e^{-\mu t}. \quad (231)$$

In order to evaluate the damping constant μ we set $\mu=\mu_r/2+i\mu_i$ and find with sufficient accuracy

$$\mu_i=-\tfrac{1}{4}|R|^2[(\nu-\omega)/\{(\nu-\omega)^2+\tfrac{1}{4}\gamma^2\}-(\nu+\omega)/\{(\nu+\omega)^2+\tfrac{1}{4}\gamma^2\}], \quad (232)$$

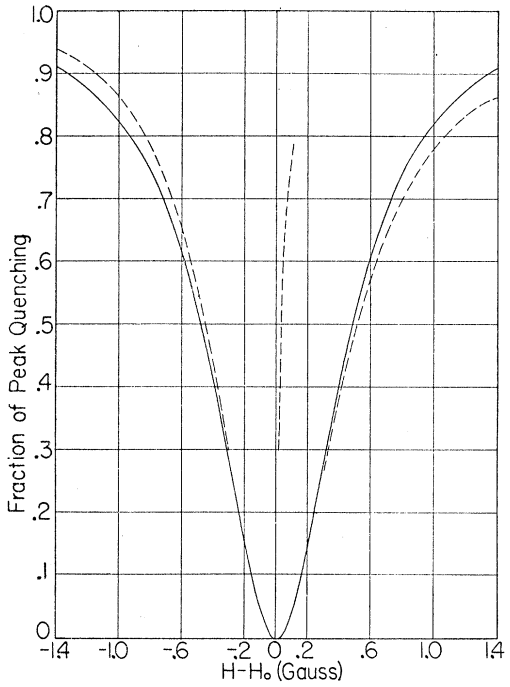

FIG. 53. Form of $\alpha\beta$ resonance expected from Eq. (219) at frequencies of 1610 Mc/sec (at βe crossing) (solid curve) and 1615 Mc/sec (5 Mc/sec away from βe crossing) (dotted curve). The latter curve is slightly asymmetrical and the apparent center as a function of quenching level is shown.

$$\mu_r=\tfrac{1}{4}\gamma|R|^2[\{\nu-\omega-\mu_i)^2+\tfrac{1}{4}(\gamma-\mu_r)^2\}^{-1}+\{(\nu+\omega)^2+\tfrac{1}{4}\gamma^2\}^{-1}]. \quad (233)$$

The rate of decay is given by μ_r. As indicated in Sec. 60, the antiresonant contribution is negligible. The peak position is determined by

$$\nu=\omega+\mu_i\simeq\omega-|R|^2(\nu-\omega)/\gamma^2+|R|^2/8\omega, \quad (234)$$

where ν has been replaced by ω in the denominators of (232). The second term of (234) produces no shift in peak position since it vanishes for $\nu=\omega$, but it does lead to a slight reduction[95] in half-width of relative order $|R|^2/\gamma^2$ as does the term with μ_r in the denominator of (233). The last term

$$|R|^2/8\omega$$

gives an rf quadratic Stark effect shift similar in form to that for static electric fields except for a factor $\frac{1}{8}$ which can perhaps be understood from the circumstances that the antiresonant perturbation has an amplitude $(1/2)R$ and the frequency denominator is effectively 2ω.

When the shift

$$|R|^2/8\omega$$

is written in the notation used by Bloch and Siegert, it is found to be one-half as large as theirs. This difference may be attributed to the damping of one of the states which in fact is responsible for the relative simplicity of our derivation. It can be seen from Eq. (228) that $a_1(t)$ would not be negligible if there were no damping.

The numerical value of the rf Stark shift $|R|^2/8\omega$ and the dimensionless ratio $|R|^2/\gamma^2$ will now be estimated for an rf power sufficient to give 63 percent quenching at resonance in 1.25×10^{-6}

[95] This "power sharpening" is at least in part due to mixing of the long-lived $2S$ state with the decaying $2P$ state giving a reduction of the radiative width of $2P$.

TABLE VII. Coefficients of series expansion for $G(\psi)$.

c_n	b_n
$c_1 = 0.8862269$	
$c_2 = -0.5000000$	
$c_3 = 0.2954090$	
$c_4 = -0.1014592$	$b_4 = 0.0825000$
$c_5 = -0.0295409$	
$c_6 = 0.0057894$	$b_6 = -0.0027778$
$c_7 = 0.0004689$	
$c_8 = -0.0000645$	$b_8 = 0.0000248$
$c_9 = -0.0000026$	
$c_{10} = 0.0000003$	$b_{10} = -0.00000001$

sec. This requires that

$$\mu_r = |R|^2/\gamma = 8\times 10^5 \text{ sec}^{-1}$$

so that

$$R = [(8\times 10^5)(6.25\times 10^8)]^{\frac{1}{2}} = 2.24\times 10^7 \text{ sec}^{-1}. \quad (235)$$

Then the shift

$$|R|^2/8\omega \sim 1\times 10^4 \text{ sec}^{-1} \quad (236)$$

amounts to 0.0016 Mc/sec when $\omega/2\pi = 1000$ Mc/sec which is entirely negligible. The dimensionless ratio $|R|^2/\gamma^2$ giving the "shock" damping and power sharpening[95] has the value 1.3×10^{-3} and causes no significant error.

APPENDIX V. PROPERTIES OF $G(\psi)$

The integral

$$G(\psi) = 2\int_0^\infty [1-\exp(-\psi/z)]e^{-z^2}z^3 dz \quad (237)$$

of Sec. 62 obeys the differential equation

$$(\psi/2)G''' - G'' + G - 1 = 0 \quad (238)$$

with boundary conditions at the regular singular point $\psi = 0$, $G(0) = 0$, $G'(0) = (1/2)(\pi)^{\frac{1}{2}}$, $G''(0) = -1/2$, and $G'''(0) = (1/6)(\pi)^{\frac{1}{2}}$, while $G(\infty) = 1$. The fourth and higher derivatives of G are infinite at $\psi = 0$, and one finds an expansion about that point in the form

$$G(\psi) = \sum_{n=1}^{\infty} c_n \psi^n + (\log\psi) \sum_{n=4}^{\infty} b_n \psi^n \quad (239)$$

with coefficients as given in Table VII.

The series converges rapidly for the values of ψ needed in the experiment. For very large ψ the saddle point approximation to (237) may be used

$$G(\psi) \sim 1 - (\pi/3)^{\frac{1}{2}}\psi \exp[-3(\psi/2)^{\frac{2}{3}}]. \quad (240)$$

The relative unimportance of the exact form of velocity distribution is shown in Fig. 48 where $G(\psi)$ is compared to the functions resulting from two other plausible assumptions. The first

$$g(\psi) = 1 - \exp[-\tfrac{1}{2}\pi^{\frac{1}{2}}\psi] \quad (241)$$

would describe the quenching if all atoms had a velocity $V = \frac{1}{2}\pi^{\frac{1}{2}}U$ equal to the reciprocal average reciprocal velocity. The second function $H(\psi)$ shows the quenching if the recoil at threshold for hydrogen is taken into account.

The differences are not great, but the functions had to be calculated to be sure of this. In addition, the related function $G'''(\psi)$ plays a more significant role in discussion of similar experiments on singly ionized helium.

APPENDIX VI. MISCELLANEOUS ENERGY LEVEL CORRECTIONS

(*a*) *Finite Size of Deuteron.* The finite size of the deuteron leads to an elevation of $2S$ relative to $2P$ by an amount

$$(1/48)\alpha^4 hcR(\hbar^2/Mr_0^2 I), \quad (242)$$

where I is the binding energy of the deuteron and $r_0 = \alpha^2 a_0$ is the classical electron radius. For simplicity, a zero range wave function has been used for the deuteron. Numerically, this shift amounts to +0.45 Mc/sec, and will be contained in the experimentally determined value of S for deuterium. The same will be true of the other corrections of order S/M such as that mentioned in reference 80.

Since the deuteron has a quadrupole moment, $Q = 2.73\times 10^{-27}$ cm^2 there are also contributions to the energy of $2^2P_{\frac{3}{2}}$, of an amount

$$(1/40)(Q/r_0^2)\alpha^4 hcR[m_J^2 - (5/4)][m_I^2 - (2/3)]. \quad (243)$$

At most this energy amounts to 0.006 Mc/sec and may be neglected.

(*b*) *Meson Cloud about Nucleus.* Slotnick and Heitler[96] have shown that the distribution of mesons about a proton gives a $2S$ level shift of about 0.02 Mc/sec according to a typical meson theory consistent with observations on the electron-neutron interaction.

(*c*) *Correction to Hyperfine Structure Splitting.* The hyperfine structure for $n = 2$ has been expressed in Sec. 56 as a multiple of Δw, the splitting for $2^2S_{\frac{1}{2}}$. This in turn was taken to be one-eighth of the hyperfine splitting for $1^2S_{\frac{1}{2}}$ as measured by Prodell and Kusch.[83] Any correction due to the difference in binding ought to be far below the level of accuracy needed here. Another neglect involved the replacement of the coefficient 2 of $\mathbf{I}\cdot\mathbf{L}$ in Eq. (177) by g_S. This implies a correction to Eq. (177) of

$$(J|w_{11}'|J) = -(g_S - 2)[\Delta w/(I+\tfrac{1}{2})]m_I m_J \cdot \begin{cases} 1/12 & 2^2P_{\frac{1}{2}} \\ 1/24 & 2^2P_{\frac{3}{2}} \end{cases} \quad (244)$$

but it amounts at most to 0.013 Mc/sec, and has been neglected.

[96] M. Slotnick and W. Heitler, Phys. Rev. **75**, 1645 (1949).